Available online at www.sciencedirect.com

ScienceDirect

Nuclear Physics B 955 (2020) 115042

NUCLEAR PHYSICS B

www.elsevier.com/locate/nuclphysb

Angular momentum of the electron: One-loop studies

Bogdan Damski

Jagiellonian University, Institute of Theoretical Physics, Łojasiewicza 11, 30-348 Kraków, Poland

Received 19 December 2019; received in revised form 15 April 2020; accepted 28 April 2020
Available online 6 May 2020
Editor: Stephan Stieberger

Abstract

We combine bare perturbation theory with the imaginary time evolution technique to study one-loop radiative corrections to various components of angular momentum of the electron. Our investigations are based on the canonical decomposition of angular momentum, where spin and orbital components, associated with fermionic and electromagnetic degrees of freedom, are individually approached. We use for this purpose quantum electrodynamics in the general covariant gauge and develop a formalism, based on the repeated use of the Sochocki-Plemelj formula, for proper enforcement of the imaginary time limit. It is then shown that careful implementation of imaginary time evolutions is crucial for getting a correct result for total angular momentum of the electron in the bare perturbative expansion. We also analyze applicability of the Pauli-Villars regularization to our problem, developing a variant of this technique based on modifications of studied observables by subtraction of their ghost operator counterparts. It is then shown that such an approach leads to the consistent regularization of all angular momenta that we compute.
© 2020 The Author(s). Published by Elsevier B.V. This is an open access article under the CC BY license (http://creativecommons.org/licenses/by/4.0/). Funded by SCOAP^3.

1. Introduction

The electron, undoubtedly one of the most fundamental constituents of matter, is characterized by a set of physical properties such as the mass, charge, magnetic moment, and spin.

Experimental studies of its mass and charge, m and e below, started in the late nineteenth century in a series of experiments conducted by Thomson [1]. They have been successfully continued ever since. By contrast, progress in theoretical characterization of these parameters is rather uninspiring, if we notice that dimensionless quantities involving them–such as the fine

E-mail address: bogdan.damski@uj.edu.pl.

https://doi.org/10.1016/j.nuclphysb.2020.115042
0550-3213/© 2020 The Author(s). Published by Elsevier B.V. This is an open access article under the CC BY license (http://creativecommons.org/licenses/by/4.0/). Funded by SCOAP^3.

structure constant or ratios of the electron mass to other lepton masses–have never been convincingly estimated.

The electron's intrinsic magnetic moment was introduced by Uhlenbeck and Goudsmit [2] about a century ago in an attempt to explain the anomalous Zeeman effect, which was discovered by Preston at the same time Thomson conducted his electron experiments [3]. Its understanding rapidly progressed soon after thanks to Dirac [4], whose theory predicted

$$\frac{e}{2m} \tag{1}$$

for the electron's magnetic moment. Two decades later [5], Schwinger found a more accurate approximation through a perturbative quantum electrodynamics (QED) calculation replacing (1) with

$$\frac{e}{2m}\left(1+\frac{\alpha}{2\pi}\right), \tag{2}$$

where

$$\alpha = \frac{e^2}{4\pi} \tag{3}$$

is the fine structure constant written here in the Heaviside-Lorentz system of units combined with $\hbar = c = 1$ (we use such units throughout this work). This prediction immediately explained spectroscopic "anomalies" found in measurements of Nafe and Nelson [6] and Foley and Kusch [7] that were done concurrently with Schwinger's calculations. Ever since perturbative calculations of the electron's magnetic moment have gone hand in hand with various experimental measurements reaching astonishing accuracy [8]. These efforts allowed for some of the most stringent tests of QED.

The electron's spin was introduced together with its intrinsic magnetic moment in [2]. It was then put on a firm theoretical basis by Dirac [4], whose relativistic quantum mechanics leads to the following expression for the angular momentum operator [9]

$$\frac{1}{2}\int d^3z :\psi^\dagger \Sigma^i \psi: -\mathrm{i}\int d^3z \varepsilon^{imn} z^m :\psi^\dagger \partial_n \psi:, \tag{4}$$

where ψ is the Dirac field operator, :: denotes normal ordering,

$$\Sigma^i = \mathrm{i}\varepsilon^{imn}\gamma^m\gamma^n/2, \tag{5}$$

and γ are Dirac matrices. The first (second) operator in (4) is the fermionic spin (orbital) angular momentum operator. Consider now the electron at rest, whose spin is polarized in the $\pm z$ direction. The expectation value of operator (4), in the corresponding quantum state $|\Psi\rangle$, is $s_z\delta^{i3}$, where

$$s_z = \pm\frac{1}{2} \tag{6}$$

reflects the fact that the electron's spin equals one-half. The orbital component of the angular momentum operator does not contribute to such an expectation value

$$\left\langle -\mathrm{i}\int d^3z \varepsilon^{imn} z^m :\psi^\dagger \partial_n \psi: \right\rangle_\Psi = 0, \tag{7}$$

and so one finds

$$\left\langle \frac{1}{2} \int d^3z :\psi^\dagger \Sigma^i \psi: \right\rangle_\Psi = s_z \delta^{i3}. \tag{8}$$

The situation is considerably more complex in QED, where the total angular momentum operator is built of not only fermionic but also electromagnetic operators. The question of how one can attribute angular momentum to different degrees of freedom is non-trivial and it leads to the so-called angular momentum controversy involving various issues such as the lack of gauge invariant definition of spin and orbital angular momentum of photons and the question of experimental relevance of gauge non-invariant quantities [10]. More importantly, in the context of this work, all components of total angular momentum of the electron receive radiative corrections [11–14].

The interest in angular momentum decompositions of the electron in particular and other subatomic particles in general comes from the fact that they provide fundamental insights into properties of these particles. This statement is perhaps best illustrated by experimental and theoretical studies of angular momentum decompositions of nucleons performed over last four decades and comprehensively summarized in [15].

It is the purpose of this work to compute radiative corrections to right-hand sides of (7) and (8) as well as to remaining components of total angular momentum of the electron. Similar studies were performed not long ago [12,13]. These calculations were done in the light-front formalism, employed the light-cone gauge, and used renormalized perturbation theory. They are, on the technical level, very different from our studies as we use imaginary time evolution formalism, work in the general covariant gauge, and employ bare perturbation theory. Therefore, we see our work as complementary to previous efforts. Among other things, this paper discusses non-trivial results on implementation of imaginary time evolutions, it presents gauge non-invariant angular momenta from the covariant-gauge perspective, and it conclusively describes intricacies of proper application of the Pauli-Villars regularization to the studied problem. Its outline is the following.

We explain in Sec. 2 the approach that we use to carry out computations. Next, we describe in Sec. 3 different contributions to fermionic spin angular momentum of the electron. Remaining angular momenta–fermionic orbital, electromagnetic spin and orbital, and gauge-fixing ones–are discussed in Sec. 4. Then, a proper way of imposing the Pauli-Villars regularization onto all these expressions is presented in Sec. 5. One-loop radiative corrections are computed in Sec. 6. The discussion of obtained results is presented in Sec. 7. Several appendices are added to this paper to make its main body better readable and to facilitate verification of our calculations. We explain our notation in Appendix A and collect all bispinor matrix elements in Appendix B. Intricacies associated with implementation of imaginary time evolutions are discussed in Appendix C, while adaptation of the Pauli-Villars regularization technique to our problem is presented in Appendix D. Finally, some integrals from Sec. 6.1 are evaluated in Appendix E.

2. Basics

The starting point for our considerations is the QED Lagrangian density [9]

$$\mathcal{L} = -\frac{1}{4} F_{\mu\nu} F^{\mu\nu} + \frac{\lambda^2}{2} A_\mu A^\mu - \frac{\xi}{2} \left(\partial_\mu A^\mu\right)^2 + \overline{\psi} \left(\mathrm{i}\gamma^\mu \partial_\mu - m_\mathrm{o}\right) \psi - e_\mathrm{o} \overline{\psi} \gamma^\mu \psi A_\mu, \tag{9}$$

where the second term is employed to regulate the infrared (IR) sector of the theory, while the third one, the so-called gauge-fixing term, facilitates quantization of the electromagnetic field in the general covariant gauge (the term general refers to the arbitrary greater than zero value of ξ).

The bare mass and charge of the electron are denoted by m_o and e_o, the photon mass is written as λ, and remaining symbols follow all standard conventions (Appendix A).

We compute total angular momentum through the formula from Sec. 2.4 of [9]

$$J^i = \frac{1}{2}\varepsilon^{imn}\int d^3z M^{0mn}, \tag{10}$$

where the canonical angular momentum tensor density is given by the following sum of the orbital term, expressed through the canonical energy-momentum tensor density $\vartheta^{\mu\nu}$, and the spin term

$$M^{\mu\nu\lambda} = \vartheta^{\mu\lambda}z^\nu - \vartheta^{\mu\nu}z^\lambda + \delta M^{\mu\nu\lambda}, \tag{11a}$$

$$\begin{aligned}\vartheta^{\mu\nu} =& \frac{\partial\mathcal{L}}{\partial(\partial_\mu A^\sigma)}\partial^\nu A^\sigma + \frac{\partial\mathcal{L}}{\partial(\partial_\mu\psi)}\partial^\nu\psi - \eta^{\mu\nu}\mathcal{L} \\ =& - F^{\mu\sigma}\partial^\nu A_\sigma - \xi\partial_\sigma A^\sigma\partial^\nu A^\mu + \mathrm{i}\overline{\psi}\gamma^\mu\partial^\nu\psi - \eta^{\mu\nu}\mathcal{L},\end{aligned} \tag{11b}$$

$$\begin{aligned}\delta M^{\mu\nu\lambda} =& \frac{\partial\mathcal{L}}{\partial(\partial_\mu A^\sigma)}\left(\eta^{\nu\sigma}\eta^{\lambda\rho} - \eta^{\lambda\sigma}\eta^{\nu\rho}\right)A_\rho + \frac{\partial\mathcal{L}}{\partial(\partial_\mu\psi)}\frac{1}{4}[\gamma^\nu,\gamma^\lambda]\psi \\ =& F^{\mu\lambda}A^\nu - F^{\mu\nu}A^\lambda + \xi\partial_\sigma A^\sigma(\eta^{\mu\lambda}A^\nu - \eta^{\mu\nu}A^\lambda) + \frac{\mathrm{i}}{4}\overline{\psi}\gamma^\mu[\gamma^\nu,\gamma^\lambda]\psi,\end{aligned} \tag{11c}$$

where [,] stands for the commutator. These expressions lead to

$$\begin{aligned}J^i =& \frac{1}{2}\int d^3z\psi^\dagger\Sigma^i\psi - \mathrm{i}\int d^3z\varepsilon^{imn}z^m\psi^\dagger\partial_n\psi + \int d^3z\varepsilon^{imn}F_{m0}A_n \\ &+ \int d^3z\varepsilon^{imn}z^m F_{j0}\partial_n A_j + \xi\int d^3z\varepsilon^{imn}z^m\partial_\sigma A^\sigma\partial_n A_0.\end{aligned} \tag{12}$$

First two terms in (12), fermionic spin and orbital angular momenta, have already been introduced in Sec. 1. The third and fourth term are known as electromagnetic spin and orbital angular momenta. Finally, we will refer to the last term of (12) as gauge-fixing angular momentum because it originates from the gauge-fixing term in (9). Such a term is a unique feature of the covariant gauge approach, and so it is quite interesting to see how it contributes to total angular momentum of the electron.

The sum of first four expressions in (12) is known as the Jaffe-Manohar decomposition of total angular momentum [10,16]. As we have shown above, it follows directly from the canonical formalism, which makes it quite distinctive. Such a decomposition, however, is not unique as one can try to modify the density of angular momentum through either Euler-Lagrange equations or through addition of 3-divergence terms. Since advantages and disadvantages of different angular momentum decompositions are comprehensively discussed in [10], we will not dwell on them.

Angular momentum operators are now obtained by replacing classical fields in (12) with Heisenberg-picture operators and by imposing normal ordering. In the form suitable for perturbative calculations, we write them as

$$J^i_{\text{spin}\bullet} = \int d^3z :\overline{\psi}\,\Gamma^i\psi:,\ \ \Gamma^i = \frac{\mathrm{i}}{4}\varepsilon^{imn}\gamma^0\gamma^m\gamma^n, \tag{13}$$

$$J^i_{\text{orb}\bullet} = \int d^3z :\overline{\psi}\,\nabla^i_z\psi:,\ \ \nabla^i_z = -\mathrm{i}\gamma^0\varepsilon^{imn}z^m\frac{\partial}{\partial z^n}, \tag{14}$$

$$J^i_{\text{spin}\sim} = \int d^3z\varepsilon^{imn} :F_{m0}A_n:, \tag{15}$$

$$J^i_{\text{orb}\sim} = \int d^3z\varepsilon^{imn}z^m :F_{j0}\partial_n A_j:, \tag{16}$$

$$J^i_\xi = \xi \int d^3z\varepsilon^{imn}z^m :\partial_\sigma A^\sigma \partial_n A_0:, \tag{17}$$

where we have used the bullet $\bullet$ and the wavy line $\sim$ to distinguish fermionic operators from electromagnetic ones. The total angular momentum operator is then

$$J^i = J^i_{\text{spin}\bullet} + J^i_{\text{orb}\bullet} + J^i_{\text{spin}\sim} + J^i_{\text{orb}\sim} + J^i_\xi. \tag{18}$$

We will compute expectation values of operators (13)–(17) in the QED ground state with one net electron,[1] which we denote as $|\mathbf{\Omega}s\rangle$. As such quantities are time-independent, we set

$$z = (0, \boldsymbol{z}) \tag{19}$$

to simplify the discussion in intermediate steps (as a self-consistency check, we have verified that z^0 eventually drops out from all expectation values if it is not set to zero). Calculations will be performed in the framework of bare perturbation theory combined with the imaginary time evolution technique.

Imaginary time evolutions start from the one-electron ground state of the free Hamiltonian

$$|\mathbf{0}s\rangle = a^\dagger_{\mathbf{0}s}|0\rangle, \tag{20}$$

where $|0\rangle$ is the vacuum state of the free theory and the operator $a_{\mathbf{0}s}$ is introduced in Appendix A. Such a state describes the electron at rest whose spin is polarized such that $\langle J^i\rangle_{\mathbf{0}s} = s_z\delta^{i3}$ (the same polarization has been employed in Sec. 1). Its 4-momentum

$$f = (m_o, \mathbf{0}) \tag{21}$$

frequently appears in the following discussion. State (20) is then evolved in time (its non-trivial dynamics is induced by the interaction Hamiltonian $\int d^3x\mathcal{H}_{\text{int}}$). Enforcement of the imaginary time limit leads to [17]

$$\langle \boldsymbol{J}_\chi\rangle_{\mathbf{\Omega}s} = \lim_{T\to\infty(1-\mathrm{i}0)} \langle \boldsymbol{J}_\chi\rangle^T_{\mathbf{\Omega}s}, \tag{22a}$$

$$\langle \boldsymbol{J}_\chi\rangle^T_{\mathbf{\Omega}s} = \frac{\langle \mathbf{0}s|\mathbb{T}\boldsymbol{J}^I_\chi \exp(-\mathrm{i}\int_T d^4x\mathcal{H}^I_{\text{int}})|\mathbf{0}s\rangle}{\langle \mathbf{0}s|\mathbb{T}\exp(-\mathrm{i}\int_T d^4x\mathcal{H}^I_{\text{int}})|\mathbf{0}s\rangle}, \tag{22b}$$

$$\int_T d^4x = \int_{-T}^{T} dx^0 \int d^3x, \tag{22c}$$

$$\chi = \text{spin}\bullet, \text{orb}\bullet, \text{spin}\sim, \text{orb}\sim, \xi, \tag{22d}$$

where interaction-picture operators are labeled with the index I, $\boldsymbol{J}^I_\chi$ operators are obtained by replacing Heisenberg-picture fields with their interaction-picture counterparts,[2]

$$\mathcal{H}^I_{\text{int}} = e_o :\overline{\psi}_I\gamma^\mu\psi_I: A^I_\mu, \tag{23}$$

[1] The term net refers to the fact that besides electrons in vacuum electron-positron pairs, there is one electron in such a state.

[2] This may be less obvious for operators involving time derivatives of the 4-potential A_μ–$J^i_{\text{spin}\sim}$, $J^i_{\text{orb}\sim}$, and J^i_ξ–but it can be proven there as well (see e.g. [14]).

and $\mathbb{T}$ is the time-ordering operator.

To proceed with (22), we will need fermionic

$$
\begin{aligned}
S(x-y) &= \contraction{}{\psi}{{}_I(x)}{\overline{\psi}}\psi_I(x)\overline{\psi}_I(y) = \langle 0|\mathbb{T}\psi_I(x)\overline{\psi}_I(y)|0\rangle \\
&= \mathrm{i}\int \frac{d^4p}{(2\pi)^4}\frac{\gamma\cdot p + m_{\mathrm{o}}}{p^2 - m_{\mathrm{o}}^2 + \mathrm{i}0} e^{-\mathrm{i}p\cdot(x-y)}
\end{aligned} \tag{24}
$$

and electromagnetic

$$
\begin{aligned}
D_{\mu\nu}(x-y) &= \contraction{}{A}{{}^I_\mu(x)}{A}A^I_\mu(x)A^I_\nu(y) = \langle 0|\mathbb{T}A^I_\mu(x)A^I_\nu(y)|0\rangle \\
&= -\mathrm{i}\int \frac{d^4p}{(2\pi)^4}\frac{d_{\mu\nu}(p)}{p^2 - \lambda^2 + \mathrm{i}0} e^{-\mathrm{i}p\cdot(x-y)},
\end{aligned} \tag{25a}
$$

$$
d_{\mu\nu}(p) = \eta_{\mu\nu} + \frac{1-\xi}{\xi}\frac{p_\mu p_\nu}{p^2 - \lambda^2/\xi + \mathrm{i}0} \tag{25b}
$$

propagators. The former expression is given by the standard formula, while the latter one can be either derived using the trick from Sec. 7.6 of [9] or taken from Sec. 33.4 of [18].

Evaluation of (22b) will be performed with $T > 0$ and then the limit

$$
T \to \infty(1 - \mathrm{i}0) \tag{26}
$$

will be taken. Proper computation of this limit is no trivial matter in some of our computations. To illustrate the subtle point here, we note that integration over time in (22b) leads to expressions of the form

$$
\int_{-T}^{T} \frac{dx^0}{2\pi} e^{\mathrm{i}x^0 P^0} = \frac{\sin(TP^0)}{\pi P^0}, \tag{27}
$$

where P^0 is some combination of timelike components of 4-momenta. Limit (26) cannot be taken on (27). The standard textbook solution of this complication is to transfer the $-\mathrm{i}0$ from the limit to the imaginary part of propagators' denominators (see e.g. Sec. 4.4 of [17]). After that, the limit $T \to \infty$ is taken. This leads to the Dirac delta function due to the following well-known identity

$$
\delta(P^0) = \lim_{T\to\infty} \frac{\sin(TP^0)}{\pi P^0}. \tag{28}
$$

Such a procedure presumably greatly simplifies calculations. However, it leads to the incorrect result for fermionic spin angular momentum of the electron and it actually complicates a bit the discussion of its fermionic orbital angular momentum. Therefore, a more rigorous approach is needed and we develop it in Appendix C. Among other things, such an approach can be used for showing that the above-mentioned heuristic procedure provides correct results for other angular momenta that we discuss.

Next, we note that due to the commutation of the total angular momentum operator with the Hamiltonian, angular momentum in states $|\mathbf{0}s\rangle$ and $|\mathbf{\Omega}s\rangle$ is the same, consequently

$$
\langle J^i\rangle_{\mathbf{\Omega}s} = s_z\delta^{i3}. \tag{29}
$$

Furthermore, the expectation value of each individual angular momentum operator, say J^i_χ with χ given by (22d), must be either directly proportional to $s_z\delta^{i3}$ or vanish. It is so because after averaging over spin projections of the electron, there is no preferred direction in the three-dimensional space, where $\langle J^i_\chi\rangle_{\mathbf{\Omega}s}$ is discussed. Hence, $\langle J^i_\chi\rangle_{\mathbf{\Omega}s}$ cannot have the s_z-independent component.[3] We will use this observation over and over again to simplify calculations.

Moreover, since we will be doing the perturbative expansion around the one-electron state, we will be encountering the normalizing constant

$$V = \langle \mathbf{0}s|\mathbf{0}s\rangle = \int \frac{d^3x}{(2\pi)^3}. \tag{30}$$

While such a constant is formally infinite, it gets unambiguously cancelled during computations. This happens because all expressions that contribute to the final result describe processes that happen homogeneously in space. As a result, the outermost spatial integral in every such expression is done over a function that is constant in space, and so it exactly cancels down normalizing constant (30) appearing in the denominator of such an expression. Needless to say, factors like (30) are frequently encountered in studies involving delocalized states (see e.g. above-cited [10]).

We also mention that we will draw position-space Feynman diagrams in Figs. 1–4 to illustrate contributions to fermionic spin and orbital angular momenta of the electron. The diagram from Fig. X will be referred to as Diag. X. Rules for drawing these diagrams can be deduced without much effort by comparing them to analytical expressions that we list for them. There is no need to linger over these rules because all diagrams will be drawn only after analytical expressions will be worked out.

Finally, for the sake of brevity, we will drop the term

$$O(e_{\mathrm{o}}^4) \tag{31}$$

from all expressions for expectation values of angular momentum operators.

3. Perturbative expansion for fermionic spin angular momentum

We will derive here the IR-regularized expression for fermionic spin angular momentum of the electron. To proceed, we expand (22b) in the series in e_{o}

$$\langle \boldsymbol{J}_{\mathrm{spin}\bullet}\rangle^T_{\mathbf{\Omega}s} = \frac{\langle \mathbf{0}s|\boldsymbol{J}^I_{\mathrm{spin}\bullet}|\mathbf{0}s\rangle}{V} \tag{32a}$$

$$- \frac{1}{2}\frac{\langle \mathbf{0}s|\mathbb{T}\boldsymbol{J}^I_{\mathrm{spin}\bullet}\int_T d^4x\mathcal{H}^I_{\mathrm{int}}\int_T d^4y\mathcal{H}^I_{\mathrm{int}}|\mathbf{0}s\rangle}{V} \tag{32b}$$

$$+ \frac{1}{2}\frac{\langle \mathbf{0}s|\boldsymbol{J}^I_{\mathrm{spin}\bullet}|\mathbf{0}s\rangle}{V}\frac{\langle \mathbf{0}s|\mathbb{T}\int_T d^4x\mathcal{H}^I_{\mathrm{int}}\int_T d^4y\mathcal{H}^I_{\mathrm{int}}|\mathbf{0}s\rangle}{V}. \tag{32c}$$

Zeroth-order contribution (32a) is illustrated in Fig. 1. We obtain after using (A.4) and (A.5)

$$\frac{\langle \mathbf{0}s|(\boldsymbol{J}^I_{\mathrm{spin}\bullet})^i|\mathbf{0}s\rangle}{V} = \frac{\overline{u}_s\Gamma^i u_s}{V}\int\frac{d^3z}{(2\pi)^3} = s_z\delta^{i3}. \tag{33}$$

[3] As a self-consistency check, we have directly verified for $\xi = 1$ that this is indeed the case in all our calculations. The same explicit verification has been also performed for expectation values of ghost operators $\tilde{J}^i_\chi$ discussed in Appendix D.

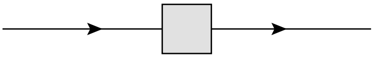

Fig. 1. Diagrammatic illustration of $\overline{u}_s\Gamma^i u_s/(2\pi)^3$ from (33). The grey box stands for the operator Γ^i from (13). External lines are for zero-momentum electrons (the same notation is used in all our figures).

To compute (32b), we need the following matrix element that can be obtained through Wick's theorem combined with (A.4)

$$\langle \mathbf{0}s|\mathbb{T}:\overline{\psi}_I(z)\Gamma^i\psi_I(z)::\overline{\psi}_I(x)\gamma^\mu\psi_I(x)::\overline{\psi}_I(y)\gamma^\nu\psi_I(y):|\mathbf{0}s\rangle =$$

$$\frac{e^{\mathrm{i}f\cdot(x-y)}}{(2\pi)^3}\overline{u}_s\gamma^\mu S(x-z)\Gamma^i S(z-y)\gamma^\nu u_s \tag{34a}$$

$$+\frac{e^{\mathrm{i}f\cdot(z-y)}}{(2\pi)^3}\overline{u}_s\Gamma^i S(z-x)\gamma^\mu S(x-y)\gamma^\nu u_s \tag{34b}$$

$$+\frac{e^{\mathrm{i}f\cdot(x-z)}}{(2\pi)^3}\overline{u}_s\gamma^\mu S(x-y)\gamma^\nu S(y-z)\Gamma^i u_s \tag{34c}$$

$$-\frac{1}{2(2\pi)^3}\mathrm{Tr}\big[S(y-x)\gamma^\mu S(x-y)\gamma^\nu\big]\overline{u}_s\Gamma^i u_s \tag{34d}$$

$$-\frac{1}{(2\pi)^3}\mathrm{Tr}\Big[S(y-z)\Gamma^i S(z-y)\gamma^\nu\Big]\overline{u}_s\gamma^\mu u_s \tag{34e}$$

$$-V\,\mathrm{Tr}\Big[S(x-z)\Gamma^i S(z-y)\gamma^\nu S(y-x)\gamma^\mu\Big] \tag{34f}$$

$$+(x,\mu\leftrightarrow y,\nu \text{ on all terms}). \tag{34g}$$

Matrix element (34) can be additionally simplified with (19) and (21) leading to $e^{\mathrm{i}f\cdot z}=1$. Its contractions with the photon propagator are diagrammatically depicted in Fig. 2.

To compute (32c), we proceed similarly as in (34) getting

$$\frac{\langle \mathbf{0}s|:\overline{\psi}_I(z)\Gamma^i\psi_I(z):|\mathbf{0}s\rangle}{V}\langle \mathbf{0}s|\mathbb{T}:\overline{\psi}_I(x)\gamma^\mu\psi_I(x)::\overline{\psi}_I(y)\gamma^\nu\psi_I(y):|\mathbf{0}s\rangle =$$

$$\frac{e^{\mathrm{i}f\cdot(x-y)}}{(2\pi)^6}\frac{\overline{u}_s\Gamma^i u_s}{V}\overline{u}_s\,\gamma^\mu S(x-y)\gamma^\nu u_s \tag{35a}$$

$$-\frac{1}{2(2\pi)^3}\mathrm{Tr}\big[S(y-x)\gamma^\mu S(x-y)\gamma^\nu\big]\overline{u}_s\Gamma^i u_s \tag{35b}$$

$$+(x,\mu\leftrightarrow y,\nu \text{ on all terms}), \tag{35c}$$

whose contractions with the photon propagator are diagrammatically shown in Fig. 3. Replacements (34g) and (35c) produce a factor of 2 during evaluation of diagrams, which cancels down a prefactor of $1/2$ from (32b) and (32c).

To correctly evaluate contributions of different diagrams to fermionic spin angular momentum of the electron, one must properly enforce limit (26). This has to be carefully done because the standard procedure outlined between (27) and (28) leads to incorrect results when Diags. 2b, 2c, and 3a are considered. The comprehensive discussion of the appropriate way of handling the imaginary time limit can be found in Appendix C. We will frequently refer the reader to it quoting below only its final outcomes for individual diagrams.

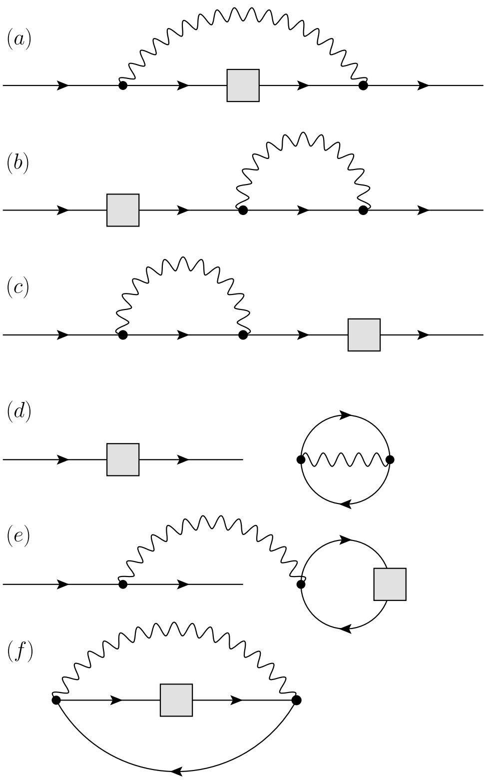

Fig. 2. The (a)–(f) panels illustrate photon-propagator contractions with expressions (34a)–(34f), respectively.

Finally, to make equations a bit more compact, we introduce the following notation

$$\text{Diag. X} = \lim_{T\to\infty(1-\mathrm{i}0)} \text{Diag. X}|_T\,, \tag{36}$$

$$\tilde{q} = (q^0, \boldsymbol{p}),\ \bar{k} = (k^0, -\boldsymbol{p}). \tag{37}$$

We are now ready to discuss diagrams.

Diagram 3a. We start with

$$\begin{aligned}\text{Diag. 3a}|_T &= \frac{e_\mathrm{o}^2}{V^2}\int \frac{d^3z}{(2\pi)^3}\overline{u}_s\Gamma^i u_s \int_T d^4x d^4y \frac{e^{\mathrm{i}f\cdot(x-y)}}{(2\pi)^3} D_{\mu\nu}(x-y)\overline{u}_s\gamma^\mu S(x-y)\gamma^\nu u_s \\ &= \frac{e_\mathrm{o}^2 s_z\delta^{i3}}{(2\pi)^3 V}\int_T d^4x d^4y \int \frac{d^4p}{(2\pi)^4}\frac{d^4k}{(2\pi)^4}\frac{e^{\mathrm{i}(f-k-p)\cdot(x-y)}}{k^2-\lambda^2+\mathrm{i}0}\frac{\overline{u}_s\gamma^\mu(\gamma\cdot p+m_\mathrm{o})\gamma^\nu u_s}{p^2-m_\mathrm{o}^2+\mathrm{i}0}d_{\mu\nu}(k) \\ &= 2e_\mathrm{o}^2 s_z\delta^{i3}\int \frac{d^4p}{(2\pi)^4}dk^0 F(k^0,p^0)\frac{\sin^2[T(k^0+p^0-m_\mathrm{o})]}{(k^0+p^0-m_\mathrm{o})^2},\end{aligned} \tag{38}$$

where identities (B.1) and (B.2) have been employed to get

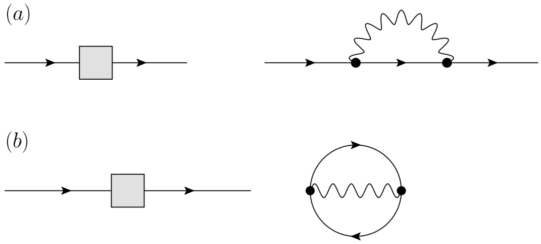

Fig. 3. The (a) and (b) panels illustrate photon-propagator contractions with expressions (35a) and (35b), respectively.

$$F(k^0,p^0)=\frac{2}{\pi}\frac{2m_o-p^0}{(\bar{k}^2-\lambda^2+\mathrm{i}0)(p^2-m_o^2+\mathrm{i}0)} + \frac{1-\xi}{\pi\xi}\frac{2k^0\bar{k}\cdot p+\bar{k}^2(m_o-p^0)}{(\bar{k}^2-\lambda^2+\mathrm{i}0)(\bar{k}^2-\lambda^2/\xi+\mathrm{i}0)(p^2-m_o^2+\mathrm{i}0)}. \tag{39}$$

Note that we only list those arguments of the function F that are most relevant for enforcement of the imaginary time limit. Using (C.8), we get

$$\text{Diag. 3a} = 2\pi e_o^2 s_z\delta^{i3}\int\frac{d^4p}{(2\pi)^4}F(m_o-p^0,p^0)\lim_{T\to\infty(1-\mathrm{i}0)}T \tag{40a}$$

$$+\frac{e_o^2 s_z\delta^{i3}}{2}\int\frac{d^4p}{(2\pi)^4}dk^0\left[\frac{F(k^0,p^0)}{(k^0+p^0-m_o+\mathrm{i}0)^2}+\frac{F(k^0,p^0)}{(k^0+p^0-m_o-\mathrm{i}0)^2}\right]. \tag{40b}$$

It is now worth to stress that the procedure described between (27) and (28) produces the following ill-defined factor under the integral sign

$$[\delta(k^0+p^0-m_o)]^2, \tag{41}$$

which gives a warning sign that such a simplification is meaningless in this case. By ignoring this fact, one ends with term (40a) after a formal identification of $\delta(0)$ with

$$\lim_{T\to\infty(1-\mathrm{i}0)}\int_{-T}^{T}\frac{dx^0}{2\pi}. \tag{42}$$

Leaving aside the discussion of this dubious substitution, such a procedure *misses* crucially-important term (40b), whose derivation requires a more sophisticated analytical approach (Appendix C). We also mention that (40a) cancels out with similar terms from Diags. 2b and 2c.[4]

Diagrams 2b and 2c. Now, we compute

$$\text{Diag. 2b}|_T = -\frac{e_o^2}{V}\int_T d^4x d^4y\int\frac{d^3z}{(2\pi)^3}e^{\mathrm{i}f\cdot(z-y)}D_{\mu\nu}(x-y)\overline{u}_s\Gamma^i S(z-x)\gamma^\mu S(x-y)\gamma^\nu u_s$$

$$= -\frac{\mathrm{i}e_o^2}{V}\int_T d^4x d^4y\int\frac{d^3z}{(2\pi)^3}\int\frac{d^4k}{(2\pi)^4}\frac{d^4p}{(2\pi)^4}\frac{d^4q}{(2\pi)^4}\frac{e^{\mathrm{i}(q-k-p)\cdot x+\mathrm{i}(k+p-f)\cdot y+\mathrm{i}(f-q)\cdot z}}{k^2-\lambda^2+\mathrm{i}0}$$

[4] The sum of Diags. 2b, 2c, and 3a is entirely determined by careful enforcement of limit (26). It cannot be obtained by the simplified procedure mentioned between (27) and (28).

$$\cdot \frac{\overline{u}_s \Gamma^i (\gamma \cdot q + m_\mathrm{o}) \gamma^\mu (\gamma \cdot p + m_\mathrm{o}) \gamma^\nu u_s}{(q^2 - m_\mathrm{o}^2 + \mathrm{i}0)(p^2 - m_\mathrm{o}^2 + \mathrm{i}0)} d_{\mu\nu}(k). \tag{43}$$

Employing (B.3) and (B.4), (43) can be written as

$$\begin{aligned}&\text{Diag. 2b}|_T = -2\mathrm{i} e_\mathrm{o}^2 s_z \delta^{i3} \\ &\cdot \int \frac{d^4 p}{(2\pi)^4} \frac{dq^0 dk^0}{2\pi} \frac{F(k^0, p^0)}{q^0 - m_\mathrm{o} + \mathrm{i}0} \frac{\sin[T(k^0 + p^0 - q^0)]}{k^0 + p^0 - q^0} \frac{\sin[T(k^0 + p^0 - m_\mathrm{o})]}{k^0 + p^0 - m_\mathrm{o}}.\end{aligned} \tag{44}$$

We now note that the procedure outlined between (27) and (28) leads to $\delta(q^0 - m_\mathrm{o})$ producing a meaningless factor of $1/\mathrm{i}0$ in the expression for Diag. 2b. This leaves no doubts that careful implementation of the imaginary time limit is necessary.

So, using (C.15), we find

$$\begin{aligned}\text{Diag. 2b} = &-\pi e_\mathrm{o}^2 s_z \delta^{i3} \int \frac{d^4 p}{(2\pi)^4} F(m_\mathrm{o} - p^0, p^0) \lim_{T\to\infty(1-\mathrm{i}0)} T \\ &- \frac{e_\mathrm{o}^2 s_z \delta^{i3}}{2} \int \frac{d^4 p}{(2\pi)^4} dk^0 \frac{F(k^0, p^0)}{(k^0 + p^0 - m_\mathrm{o} - \mathrm{i}0)^2}.\end{aligned} \tag{45}$$

Computation of

$$\text{Diag. 2c}|_T = -\frac{e_\mathrm{o}^2}{V} \int_T d^4x d^4y \int \frac{d^3 z}{(2\pi)^3} e^{\mathrm{i} f\cdot(x-z)} D_{\mu\nu}(x-y) \overline{u}_s \gamma^\mu S(x-y) \gamma^\nu S(y-z) \Gamma^i u_s \tag{46}$$

follows now straightforwardly as through formal manipulations one can show that

$$\text{Diag. 2c} = \text{Diag. 2b} \tag{47}$$

if (19) holds.

Diagram 2a. We compute here

$$\begin{aligned}\text{Diag. 2a}|_T &= -\frac{e_\mathrm{o}^2}{V} \int_T d^4x d^4y \int \frac{d^3 z}{(2\pi)^3} e^{\mathrm{i} f\cdot(x-y)} D_{\mu\nu}(x-y) \overline{u}_s \gamma^\mu S(x-z) \Gamma^i S(z-y) \gamma^\nu u_s \\ &= -\frac{\mathrm{i} e_\mathrm{o}^2}{V} \int_T d^4x d^4y \int \frac{d^3 z}{(2\pi)^3} \int \frac{d^4 k}{(2\pi)^4} \frac{d^4 p}{(2\pi)^4} \frac{d^4 q}{(2\pi)^4} \frac{e^{\mathrm{i}(f-k-p)\cdot x + \mathrm{i}(k+q-f)\cdot y + \mathrm{i}(p-q)\cdot z}}{k^2 - \lambda^2 + \mathrm{i}0} \\ &\quad \cdot \frac{\overline{u}_s \gamma^\mu (\gamma \cdot p + m_\mathrm{o}) \Gamma^i (\gamma \cdot q + m_\mathrm{o}) \gamma^\nu u_s}{(p^2 - m_\mathrm{o}^2 + \mathrm{i}0)(q^2 - m_\mathrm{o}^2 + \mathrm{i}0)} d_{\mu\nu}(k) \\ &= -4\mathrm{i} e_\mathrm{o}^2 \int \frac{d^4 p}{(2\pi)^4} \frac{dk^0 dq^0}{(2\pi)^2} \frac{\overline{u}_s \gamma^\mu (\gamma \cdot p + m_\mathrm{o}) \Gamma^i (\gamma \cdot \tilde{q} + m_\mathrm{o}) \gamma^\nu u_s}{(\bar{k}^2 - \lambda^2 + \mathrm{i}0)(p^2 - m_\mathrm{o}^2 + \mathrm{i}0)(\tilde{q}^2 - m_\mathrm{o}^2 + \mathrm{i}0)} d_{\mu\nu}(\bar{k}) \\ &\quad \cdot \frac{\sin[T(k^0 + p^0 - m_\mathrm{o})]}{k^0 + p^0 - m_\mathrm{o}} \frac{\sin[T(k^0 + q^0 - m_\mathrm{o})]}{k^0 + q^0 - m_\mathrm{o}}.\end{aligned} \tag{48}$$

With the help of (B.5), (B.6), and (C.21) we arrive at

$$\begin{aligned}\text{Diag. 2a} = -\mathrm{i} e_\mathrm{o}^2 s_z \delta^{i3} \int \frac{d^4 p}{(2\pi)^4} \Bigg[&\frac{2(p^2 + m_\mathrm{o}^2) + 4(p_3)^2}{(p^2 - m_\mathrm{o}^2 + \mathrm{i}0)^2 [(p-f)^2 - \lambda^2 + \mathrm{i}0]} \\ &+ \frac{1-\xi}{\xi} \frac{1}{[(p-f)^2 - \lambda^2 + \mathrm{i}0][(p-f)^2 - \lambda^2/\xi + \mathrm{i}0]} \Bigg].\end{aligned} \tag{49}$$

We mention in passing that the procedure discussed between (27) and (28) gives a correct result here (no singularities are encountered during its implementation).

There are no other one-loop contributions to fermionic spin angular momentum of the electron in covariantly quantized QED. Indeed, disconnected vacuum bubble Diags. 2d and 3b immediately cancel out due to the difference in overall signs of (32b) and (32c). Therefore, there is no need to write down expressions for them. Moreover,

$$\text{Diag. 2e} = \lim_{T\to\infty(1-\mathrm{i}0)} \frac{e_{\mathrm{o}}^2}{V}\int_T d^4x d^4y \int \frac{d^3z}{(2\pi)^3} D_{\mu\nu}(x-y)\mathrm{Tr}\Big[S(y-z)\Gamma^i S(z-y)\gamma^\nu\Big]\overline{u}_s\gamma^\mu u_s \tag{50}$$

and

$$\text{Diag. 2f} = \lim_{T\to\infty(1-\mathrm{i}0)} e_{\mathrm{o}}^2\int_T d^4x d^4y \int d^3z D_{\mu\nu}(x-y)\mathrm{Tr}\Big[S(x-z)\Gamma^i S(z-y)\gamma^\nu S(y-x)\gamma^\mu\Big] \tag{51}$$

also do not contribute because they are both s_z-independent–see identity (B.7) and the discussion below (29).

The final IR-regularized result for fermionic spin angular momentum of the electron comes from Diags. 1, 2a–2c, and 3a

$$\langle J^i_{\mathrm{spin}\bullet}\rangle^{\lambda}_{\mathbf{\Omega}s} = \text{Diag. 1} + \text{Diag. 2a} + \text{Diag. 2b} + \text{Diag. 2c} + \text{Diag. 3a}, \tag{52}$$

where the superscript λ indicates the fact that the IR regularization is present in (52). This expression can be obtained by adding (33) and (49) to

$$\text{Diag. 2b} + \text{Diag. 2c} + \text{Diag. 3a} = 2\mathrm{i}e_{\mathrm{o}}^2 s_z\delta^{i3} \cdot\int\frac{d^4p}{(2\pi)^4}\left[\frac{\omega_{\boldsymbol{p}}^2(p^2-m_{\mathrm{o}}^2)+\lambda^2[3(p^0-m_{\mathrm{o}})^2-\omega_{\boldsymbol{p}}^2]}{\lambda^2(p^2-m_{\mathrm{o}}^2+\mathrm{i}0)[(p-f)^2-\lambda^2+\mathrm{i}0]^2} - \frac{\omega_{\boldsymbol{p}}^2+\lambda^2/\xi}{\lambda^2[(p-f)^2-\lambda^2/\xi+\mathrm{i}0]^2}\right]. \tag{53}$$

Note that there is no singularity in the integrand of (53) at $\lambda=0$ despite a factor of λ^2 in denominators, which can be shown by rearranging terms.

4. Perturbative expansion for other angular momenta

We will derive here IR-regularized expressions for fermionic orbital angular momentum, electromagnetic spin and orbital angular momenta, and gauge-fixing angular momentum.

Such an expression for fermionic orbital angular momentum can be obtained through straightforward modifications of calculations reported in Sec. 3. We will discuss its derivation in Sec. 4.1.

Results for electromagnetic spin, electromagnetic orbital, and gauge-fixing angular momenta have to be derived from scratch, which is simplified by the following observation. Namely, it can be easily shown with (C.21), that IR-regularized expressions for these angular momenta can be obtained from (22) through the replacement

$$\lim_{T\to\infty(1-\mathrm{i}0)}\int_T d^4x \to \int d^4x. \tag{54}$$

The hint that such a simplification is going to work comes from the fact that (54), which amounts to the procedure described between (27) and (28), does not lead to singular expressions here. By combining (54) with the following observation

$$\langle \mathbf{0}s|\boldsymbol{J}^I_\chi|\mathbf{0}s\rangle = \mathbf{0}, \quad \chi = \text{spin}\sim, \text{orb}\sim, \xi, \tag{55}$$

we find from (22) that

$$\langle \boldsymbol{J}_\chi\rangle_{\boldsymbol{\Omega}s} = -\frac{1}{2V}\int d^4x d^4y \langle \mathbf{0}s|\mathbb{T}\boldsymbol{J}^I_\chi \mathcal{H}^I_{\text{int}}(x)\mathcal{H}^I_{\text{int}}(y)|\mathbf{0}s\rangle, \tag{56}$$

which will be used in Secs. 4.2–4.4.

4.1. Fermionic orbital angular momentum

We begin by noting that

$$\langle \mathbf{0}s|\boldsymbol{J}^I_{\text{orb}\bullet}|\mathbf{0}s\rangle = \mathbf{0}, \tag{57}$$

which simplifies a bit the following discussion based on (22). Another matrix element that we need to know is

$$\langle \mathbf{0}s|\mathbb{T}:\overline{\psi}_I(z)\nabla^i_z\psi_I(z)::\overline{\psi}_I(x)\gamma^\mu\psi_I(x)::\overline{\psi}_I(y)\gamma^\nu\psi_I(y):|\mathbf{0}s\rangle =$$

$$\frac{e^{\mathrm{i}f\cdot(x-y)}}{(2\pi)^3}\overline{u}_s\gamma^\mu S(x-z)\nabla^i_z S(z-y)\gamma^\nu u_s \tag{58a}$$

$$+\frac{e^{\mathrm{i}f\cdot(z-y)}}{(2\pi)^3}\overline{u}_s\nabla^i_z S(z-x)\gamma^\mu S(x-y)\gamma^\nu u_s \tag{58b}$$

$$-\frac{1}{(2\pi)^3}\mathrm{Tr}\Big[S(y-z)\nabla^i_z S(z-y)\gamma^\nu\Big]\overline{u}_s\gamma^\mu u_s \tag{58c}$$

$$-V\,\mathrm{Tr}\Big[S(x-z)\nabla^i_z S(z-y)\gamma^\nu S(y-x)\gamma^\mu\Big] \tag{58d}$$

$$+(x,\mu\leftrightarrow y,\nu \text{ on all terms}), \tag{58e}$$

whose contractions with the photon propagator are diagrammatically depicted in Fig. 4. Such an expression can be obtained by replacing Γ^i in (34) by ∇^i_z and by noting that the latter operator gives zero when acting on bispinors u_s (A.5). Replacements (58e) produce a factor of 2 during evaluation of diagrams, which cancels down a prefactor of 1/2 coming from the second order expansion of the exponential function in the numerator of (22b).

Armed with (58), we can proceed similarly as in Sec. 3 discussing each diagram separately. We start from the only diagram, which yields a non-zero contribution to fermionic orbital angular momentum of the electron.

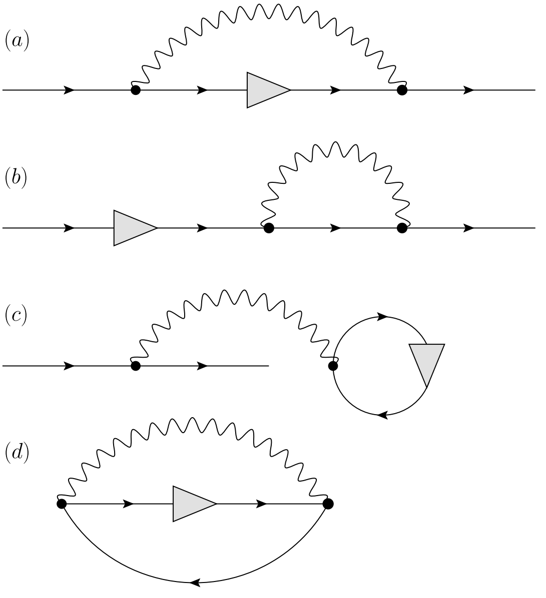

Fig. 4. The (a)–(d) panels illustrate photon-propagator contractions with expressions (58a)–(58d), respectively. The grey triangle stands for the operator ∇_z^i, which is defined in (14). It acts on the fermionic propagator attached to its vertex.

Diagram 4a. We employ notation (36) and compute

$$\text{Diag. 4a}|_T = -\frac{e_o^2}{V}\int\limits_T d^4x d^4y \int \frac{d^3z}{(2\pi)^3} e^{\mathrm{i}f\cdot(x-y)} D_{\mu\nu}(x-y)\overline{u}_s\gamma^\mu S(x-z)\nabla_z^i S(z-y)\gamma^\nu u_s$$

$$= -\mathrm{i}\frac{e_o^2}{V}\int\limits_T d^4x d^4y \int \frac{d^3z}{(2\pi)^3} \int \frac{d^4k}{(2\pi)^4}\frac{d^4p}{(2\pi)^4}\frac{d^4q}{(2\pi)^4} \frac{e^{\mathrm{i}(f-k-p)\cdot x+\mathrm{i}(k+q-f)\cdot y+\mathrm{i}(p-q)\cdot z}}{k^2-\lambda^2+\mathrm{i}0}$$

$$\cdot (\boldsymbol{z}\times\boldsymbol{q})^i \frac{\overline{u}_s\gamma^\mu(\gamma\cdot p+m_o)\gamma^0(\gamma\cdot q+m_o)\gamma^\nu u_s}{(p^2-m_o^2+\mathrm{i}0)(q^2-m_o^2+\mathrm{i}0)} d_{\mu\nu}(k). \tag{59}$$

Next, we use

$$\int \frac{d^3z}{(2\pi)^3} e^{\mathrm{i}(p-q)\cdot z}(\boldsymbol{z}\times\boldsymbol{q})^i = \varepsilon^{imn}q^n\frac{\mathrm{i}}{2}\left(\frac{\partial}{\partial p^m}-\frac{\partial}{\partial q^m}\right)\delta(\boldsymbol{p}-\boldsymbol{q}), \tag{60}$$

and integrate by parts to move derivatives acting on $\delta(\boldsymbol{p}-\boldsymbol{q})$ to the rest of the integrand. Boundary terms from integration by parts disappear. For example, because the integrand of the resulting surface integral is proportional to

$$\varepsilon^{imn}q^m q^n = 0. \tag{61}$$

Derivatives of propagators' denominators lead to the same factors and so they also do not contribute. A similar thing can be said about derivatives of the exponential term because

$$\int d^3x d^3y \delta(\boldsymbol{p}-\boldsymbol{q})\left(\frac{\partial}{\partial p^m}-\frac{\partial}{\partial q^m}\right) e^{\mathrm{i}(q\cdot y-p\cdot x)} \sim \int d^3x d^3y(\boldsymbol{x}+\boldsymbol{y})^m e^{\mathrm{i}\boldsymbol{q}\cdot(\boldsymbol{x}-\boldsymbol{y})} = 0. \tag{62}$$

In the end, after spacetime integrations and employment of (C.21), we arrive at

$$\text{Diag. 4a} = \frac{e_o^2}{2} \int \frac{d^4 p}{(2\pi)^4} \frac{\varepsilon^{imn} p^n \overline{u}_s \gamma^\mu \{\gamma^m \gamma^0, \gamma \cdot p + m_o\} \gamma^\nu u_s}{(p^2 - m_o^2 + i0)^2[(p-f)^2 - \lambda^2 + i0]} d_{\mu\nu}(f-p), \tag{63}$$

where { , } stands for the anticommutator.

Finally, we use (B.8) and (B.9) to get

$$\text{Diag. 4a} = -4ie_o^2 s_z \delta^{i3} \int \frac{d^4 p}{(2\pi)^4} \frac{(p_1)^2 + (p_2)^2}{(p^2 - m_o^2 + i0)^2[(p-f)^2 - \lambda^2 + i0]} \cdot \left(1 + \frac{1-\xi}{2\xi} \frac{p^2 - m_o^2}{(p-f)^2 - \lambda^2/\xi + i0}\right). \tag{64}$$

It is perhaps worth to mention that the procedure discussed between (27) and (28) leads to the same result for this diagram.

Diagram 4b. We study now

$$\begin{aligned} \text{Diag. 4b}|_T &= -\frac{e_o^2}{V} \int_T d^4x d^4y \int \frac{d^3z}{(2\pi)^3} e^{if\cdot(z-y)} D_{\mu\nu}(x-y) \overline{u}_s \nabla_z^i S(z-x) \gamma^\mu S(x-y) \gamma^\nu u_s \\ &= -i\frac{e_o^2}{V} \int_T d^4x d^4y \int \frac{d^3z}{(2\pi)^3} \int \frac{d^4k}{(2\pi)^4} \frac{d^4p}{(2\pi)^4} \frac{d^4q}{(2\pi)^4} \frac{e^{i(q-k-p)\cdot x + i(k+p-f)\cdot y + i(f-q)\cdot z}}{k^2 - \lambda^2 + i0} \\ &\quad \cdot (\boldsymbol{z} \times \boldsymbol{q})^i \frac{\overline{u}_s \gamma^0 (\gamma \cdot q + m_o) \gamma^\mu (\gamma \cdot p + m_o) \gamma^\nu u_s}{(q^2 - m_o^2 + i0)(p^2 - m_o^2 + i0)} d_{\mu\nu}(k). \end{aligned} \tag{65}$$

Next, we note that

$$\int \frac{d^3z}{(2\pi)^3} e^{i(f-q)\cdot z} (\boldsymbol{z} \times \boldsymbol{q})^i = -i\varepsilon^{imn} \frac{\partial}{\partial q^m} [q^n \delta(\boldsymbol{q})], \tag{66}$$

which after integration by parts, where boundary terms trivially vanish, immediately shows that Diag. $4\text{b}|_T = 0$. This implies

$$\text{Diag. 4b} = 0. \tag{67}$$

We mention in passing that such a derivation of this result avoids singular expressions that may be encountered after employment of (54).

Diagrams 4c and 4d. These diagrams,

$$\text{Diag. 4c} = \lim_{T\to\infty(1-i0)} \frac{e_o^2}{V} \int_T d^4x d^4y \int \frac{d^3z}{(2\pi)^3} D_{\mu\nu}(x-y) \text{Tr}\Big[S(y-z) \nabla_z^i S(z-y) \gamma^\nu\Big] \overline{u}_s \gamma^\mu u_s, \tag{68}$$

$$\text{Diag. 4d} = \lim_{T\to\infty(1-i0)} e_o^2 \int_T d^4x d^4y \int d^3z D_{\mu\nu}(x-y) \text{Tr}\Big[S(x-z) \nabla_z^i S(z-y) \gamma^\nu S(y-x) \gamma^\mu\Big], \tag{69}$$

do not contribute to fermionic orbital angular momentum because they are s_z-independent–see identity (B.7) and the discussion below (29).

The final IR-regularized result for fermionic orbital angular momentum is

$$\langle J^i_{\text{orb}\bullet} \rangle^\lambda_{\boldsymbol{\Omega} s} = \text{Diag. 4a}. \tag{70}$$

4.2. Electromagnetic spin angular momentum

We set $\chi = \mathrm{spin}\!\sim$ in (56) and note that the matrix element, which we need to compute, factorizes into the product of electromagnetic and fermionic matrix elements

$$\langle \mathbf{0}s|\mathbb{T}(\boldsymbol{J}^I_{\mathrm{spin}\sim})^i \mathcal{H}^I_{\mathrm{int}}(x)\mathcal{H}^I_{\mathrm{int}}(y)|\mathbf{0}s\rangle = e_{\mathrm{o}}^2 \mathcal{A}^i_{\mu\nu}(x,y)\mathcal{F}^{\mu\nu}(x,y), \tag{71a}$$

$$\mathcal{A}^i_{\mu\nu}(x,y) = \varepsilon^{imn}\int d^3z \langle 0|\mathbb{T}:F^I_{m0}(z)A^I_n(z)\!: A^I_\mu(x)A^I_\nu(y)|0\rangle, \tag{71b}$$

$$\mathcal{F}^{\mu\nu}(x,y) = \langle \mathbf{0}s|\mathbb{T}:\overline{\psi}_I(x)\gamma^\mu\psi_I(x)::\overline{\psi}_I(y)\gamma^\nu\psi_I(y)\!: |\mathbf{0}s\rangle. \tag{71c}$$

Evaluation of its fermionic part was done in [14], and we quote the final result for completeness here

$$\mathcal{F}^{\mu\nu}(x,y) = \mathcal{F}^{\mu\nu}_{\mathrm{sym}}(x,y) + \mathcal{F}^{\mu\nu}_{\mathrm{asym}}(x,y), \tag{72a}$$

$$\begin{aligned}\mathcal{F}^{\mu\nu}_{\mathrm{sym}}(x,y) =& \frac{\mathrm{i}}{(2\pi)^3}\int \frac{d^4p}{(2\pi)^4}\frac{p^\mu\eta^{\nu 0} + p^\nu\eta^{\mu 0} - p^0\eta^{\mu\nu} + m_{\mathrm{o}}\eta^{\mu\nu}}{p^2 - m_{\mathrm{o}}^2 + \mathrm{i}0} e^{\mathrm{i}(f-p)\cdot(x-y)} \\ &+ 2V\int \frac{d^4p}{(2\pi)^4}\frac{d^4q}{(2\pi)^4}\frac{p^\mu q^\nu + p^\nu q^\mu - \eta^{\mu\nu}(p\cdot q - m_{\mathrm{o}}^2)}{\big(p^2 - m_{\mathrm{o}}^2 + \mathrm{i}0\big)\big(q^2 - m_{\mathrm{o}}^2 + \mathrm{i}0\big)} e^{\mathrm{i}(p-q)\cdot(x-y)} \\ &+ (x \leftrightarrow y \text{ on all terms}),\end{aligned} \tag{72b}$$

$$\mathcal{F}^{\mu\nu}_{\mathrm{asym}}(x,y) = \frac{2s_z}{(2\pi)^3}\int \frac{d^4p}{(2\pi)^4}\frac{\varepsilon^{0\mu\nu 3}m_{\mathrm{o}} - \varepsilon^{\sigma\mu\nu 3}p_\sigma}{p^2 - m_{\mathrm{o}}^2 + \mathrm{i}0} e^{\mathrm{i}(f-p)\cdot(x-y)} - (x \leftrightarrow y). \tag{72c}$$

The above splitting is based on symmetry (anti-symmetry) of $\mathcal{F}^{\mu\nu}_{\mathrm{sym}}$ ($\mathcal{F}^{\mu\nu}_{\mathrm{asym}}$) with respect to the transformation $\mu \leftrightarrow \nu$. Another important difference between $\mathcal{F}^{\mu\nu}_{\mathrm{sym}}$ and $\mathcal{F}^{\mu\nu}_{\mathrm{asym}}$ is that the former is s_z-independent, and so it cannot contribute to the final result due to reasons explained below (29). We will thus replace $\mathcal{F}^{\mu\nu}$ below by $\mathcal{F}^{\mu\nu}_{\mathrm{asym}}$.

Electromagnetic matrix element (71b) is easily obtained through Wick's theorem combined with the following identity

$$\langle 0|\mathbb{T}\partial_\alpha A^I_\beta(x)A^I_\gamma(y)|0\rangle = \frac{\partial}{\partial x^\alpha}D_{\beta\gamma}(x-y), \tag{73}$$

which can be shown with canonical commutation relations. It reads

$$\begin{aligned}\mathcal{A}^i_{\mu\nu}(x,y) &= \varepsilon^{imn}\int d^3z\, \overbracket{F^I_{m0}(z)A^I_\mu}(x)\,\overbracket{A^I_n(z)A^I_\nu}(y) + (x,\mu \leftrightarrow y,\nu) \\ &= \int \frac{d^4p}{(2\pi)^4}\frac{dq^0}{2\pi}\frac{a^i_{\mu\nu}(p,q^0)e^{-\mathrm{i}p\cdot x + \mathrm{i}\tilde{q}\cdot y}}{(p^2 - \lambda^2 + \mathrm{i}0)(\tilde{q}^2 - \lambda^2 + \mathrm{i}0)},\end{aligned} \tag{74a}$$

$$\begin{aligned}a^i_{\mu\nu}(p,q_0) =& \mathrm{i}\varepsilon^{imn}p_m\left[\eta_{0\nu}\eta_{n\mu} - \eta_{0\mu}\eta_{n\nu} + \frac{1-\xi}{\xi}\left(\frac{q_0 p_\mu \eta_{n\nu}}{p^2 - \lambda^2/\xi + \mathrm{i}0} - \frac{p_0\tilde{q}_\nu\eta_{n\mu}}{\tilde{q}^2 - \lambda^2/\xi + \mathrm{i}0}\right)\right] \\ &+ \mathrm{i}\varepsilon^{imn}\eta_{m\mu}\eta_{n\nu}(p_0 + q_0),\end{aligned} \tag{74b}$$

where $\tilde{q}$ is defined in (37).

The IR-regularized expression for electromagnetic spin angular momentum of the electron can be then written as

$$\langle J^i_{\text{spin}\sim}\rangle^\lambda_{\mathbf{\Omega}s} = -\frac{e_\text{o}^2}{2V}\int d^4x d^4y \mathcal{A}^i_{\mu\nu}(x,y)\mathcal{F}^{\mu\nu}_\text{asym}(x,y). \tag{75}$$

After simple algebra, we end up with a rather surprisingly compact formula

$$\langle J^i_{\text{spin}\sim}\rangle^\lambda_{\mathbf{\Omega}s} = -4\mathrm{i}e_\text{o}^2 s_z\delta^{i3}\int \frac{d^4p}{(2\pi)^4}\frac{2(p^0-m_\text{o})^2-(p_1)^2-(p_2)^2}{(p^2-m_\text{o}^2+\mathrm{i}0)[(p-f)^2-\lambda^2+\mathrm{i}0]^2}. \tag{76}$$

4.3. Electromagnetic orbital angular momentum

We set $\chi = \text{orb}\sim$ in (56) and again notice that the resulting matrix element, which has to be computed, factorizes into the product of electromagnetic and fermionic matrix elements

$$\langle \mathbf{0}s|\mathbb{T}(\boldsymbol{J}^I_{\text{orb}\sim})^i\mathcal{H}^I_\text{int}(x)\mathcal{H}^I_\text{int}(y)|\mathbf{0}s\rangle = e_\text{o}^2\Big[\mathcal{B}^i_{\mu\nu}(x,y)+\mathcal{C}^i_{\mu\nu}(x,y)\Big]\mathcal{F}^{\mu\nu}(x,y), \tag{77}$$

where $\mathcal{B}^i_{\mu\nu}$ and $\mathcal{C}^i_{\mu\nu}$ will be defined below.

To compute the electromagnetic matrix element, equal to the expression in square brackets in (77), we need to evaluate

$$\begin{aligned}
&\int d^3z\, z^m\langle 0|\mathbb{T}:\partial_\alpha A^I_\beta(z)\partial_\gamma A^I_\delta(z): A^I_\mu(x)A^I_\nu(y)|0\rangle \\
&\quad= \int d^3z\, z^m\partial_\alpha \overbracket{A^I_\beta(z)A^I_\mu}(x)\partial_\gamma \overbracket{A^I_\delta(z)A^I_\nu}(y) + (x,\mu\leftrightarrow y,\nu) \\
&\quad= -\int d^3z\, z^m\frac{d^4p}{(2\pi)^4}\frac{d^4q}{(2\pi)^4}\frac{p_\alpha d_{\beta\mu}(p)}{p^2-\lambda^2+\mathrm{i}0}\frac{q_\gamma d_{\delta\nu}(q)}{q^2-\lambda^2+\mathrm{i}0}e^{-\mathrm{i}p\cdot x+\mathrm{i}q\cdot y+\mathrm{i}(p-q)\cdot z} \\
&\quad+ (x,\mu\leftrightarrow y,\nu) \\
&\quad= \int\frac{d^4p}{(2\pi)^4}\frac{dq^0}{2\pi}(\boldsymbol{x}+\boldsymbol{y})^m\left[{}_{\alpha\beta\gamma\delta}\Box_{\mu\nu}(p,\tilde{q})+{}_{\alpha\beta\gamma\delta}\Box_{\nu\mu}(\tilde{q},p)\right]e^{-\mathrm{i}p\cdot x+\mathrm{i}\tilde{q}\cdot y} \\
&\quad+ \int\frac{d^4p}{(2\pi)^4}\frac{dq^0}{2\pi}\left[{}_{\alpha\beta\gamma\delta m}\boxslash_{\mu\nu}(p,\tilde{q})-{}_{\alpha\beta\gamma\delta m}\boxslash_{\nu\mu}(\tilde{q},p)\right]e^{-\mathrm{i}p\cdot x+\mathrm{i}\tilde{q}\cdot y},
\end{aligned} \tag{78}$$

where contractions have been computed as in (73), d^3z integration has been done with

$$\int\frac{d^3z}{(2\pi)^3}z^m e^{\mathrm{i}(p-q)\cdot z} = \frac{\mathrm{i}}{2}\left(\frac{\partial}{\partial p^m}-\frac{\partial}{\partial q^m}\right)\delta(\boldsymbol{p}-\boldsymbol{q}), \tag{79}$$

integration by parts has been employed, and

$${}_{\alpha\beta\gamma\delta}\Box_{\mu\nu}(p,q) = -\frac{1}{2}\frac{p_\alpha d_{\beta\mu}(p)}{p^2-\lambda^2+\mathrm{i}0}\frac{q_\gamma d_{\delta\nu}(q)}{q^2-\lambda^2+\mathrm{i}0}, \tag{80}$$

$${}_{\alpha\beta\gamma\delta m}\boxslash_{\mu\nu}(p,q) = \frac{\mathrm{i}}{2}\left(\frac{\partial}{\partial p^m}-\frac{\partial}{\partial q^m}\right)\left(\frac{p_\alpha d_{\beta\mu}(p)}{p^2-\lambda^2+\mathrm{i}0}\frac{q_\gamma d_{\delta\nu}(q)}{q^2-\lambda^2+\mathrm{i}0}\right) \tag{81}$$

have been introduced. We mention in passing that there are no boundary terms from such integration by parts.

We obtain by combining (16), (77), and (78)

$$\mathcal{B}^i_{\mu\nu}(x,y) = \int \frac{d^4p}{(2\pi)^4}\frac{dq^0}{2\pi}(\boldsymbol{x}+\boldsymbol{y})^m\, b^i_{m\mu\nu}(p,\tilde{q})e^{-\mathrm{i}p\cdot x+\mathrm{i}\tilde{q}\cdot y}, \tag{82a}$$

$$b^i_{m\mu\nu}(p,q) = \varepsilon^{imn}\left[{}_{j0nj}\Box_{\mu\nu}(p,q) - {}_{0jnj}\Box_{\mu\nu}(p,q)\right] + (\mu\leftrightarrow\nu,\, p\leftrightarrow q), \tag{82b}$$

$$\mathcal{C}^i_{\mu\nu}(x,y) = \int \frac{d^4p}{(2\pi)^4}\frac{dq^0}{2\pi}c^i_{\mu\nu}(p,\tilde{q})e^{-\mathrm{i}p\cdot x+\mathrm{i}\tilde{q}\cdot y}, \tag{83a}$$

$$c^i_{\mu\nu}(p,q) = \varepsilon^{imn}\left[{}_{j0njm}\boxslash_{\mu\nu}(p,q) - {}_{0jnjm}\boxslash_{\mu\nu}(p,q)\right] - (\mu\leftrightarrow\nu,\, p\leftrightarrow q). \tag{83b}$$

Proceeding similarly as in Sec. 4.2, we write the IR-regularized expression for electromagnetic orbital angular momentum of the electron as

$$\langle J^i_{\mathrm{orb}\sim}\rangle^{\lambda}_{\mathbf{\Omega}s} = -\frac{e_{\mathrm{o}}^2}{2V}\int d^4x d^4y\left[\mathcal{B}^i_{\mu\nu}(x,y) + \mathcal{C}^i_{\mu\nu}(x,y)\right]\mathcal{F}^{\mu\nu}_{\mathrm{asym}}(x,y), \tag{84}$$

where the contribution of $\mathcal{B}^i_{\mu\nu}$ to (84) vanishes because it is proportional to the term that has the same structure as the right-hand side of (62). We get after simple algebra

$$\langle J^i_{\mathrm{orb}\sim}\rangle^{\lambda}_{\mathbf{\Omega}s} = -\frac{2e_{\mathrm{o}}^2 s_z}{V}\int d^4x d^4y \int \frac{d^4k}{(2\pi)^4}\frac{d^4p}{(2\pi)^4}\frac{dq^0}{(2\pi)^4}\frac{\varepsilon^{0\mu\nu3}m_{\mathrm{o}} - \varepsilon^{\sigma\mu\nu3}k_\sigma}{k^2-m_{\mathrm{o}}^2+\mathrm{i}0}c^i_{\mu\nu}(p,\tilde{q}) \cdot e^{\mathrm{i}(f-k-p)\cdot x+\mathrm{i}(k+\tilde{q}-f)\cdot y}. \tag{85}$$

Finally, with the help of

$$c^i_{\mu\nu}(p,p) = \frac{\mathrm{i}\varepsilon^{imn}p_m(\eta_{0\mu}\eta_{n\nu}-\eta_{0\nu}\eta_{n\mu})}{(p^2-\lambda^2+\mathrm{i}0)^2}\left(1-\frac{1}{2\xi}\frac{p^2-\lambda^2}{p^2-\lambda^2/\xi+\mathrm{i}0}\right), \tag{86}$$

we obtain

$$\langle J^i_{\mathrm{orb}\sim}\rangle^{\lambda}_{\mathbf{\Omega}s} = -4\mathrm{i}e_{\mathrm{o}}^2 s_z\delta^{i3}\int\frac{d^4p}{(2\pi)^4}\frac{(p_1)^2+(p_2)^2}{(p^2-m_{\mathrm{o}}^2+\mathrm{i}0)[(p-f)^2-\lambda^2+\mathrm{i}0]^2} \cdot\left[1-\frac{1}{2\xi}\frac{(p-f)^2-\lambda^2}{(p-f)^2-\lambda^2/\xi+\mathrm{i}0}\right]. \tag{87}$$

4.4. Gauge-fixing angular momentum

We set $\chi=\xi$ in (56) and note that the resulting expression can be obtained by straightforward modifications of calculations from Sec. 4.3. Namely, $\langle J^i_\xi\rangle_{\mathbf{\Omega}s}$ is given by the right-hand side of (85) with $c^i_{\mu\nu}$ being replaced by $\tilde{c}^i_{\mu\nu}$, whose diagonal components are given by

$$\tilde{c}^i_{\mu\nu}(p,p) = \frac{\mathrm{i}\varepsilon^{imn}p_m}{(p^2-\lambda^2+\mathrm{i}0)(p^2-\lambda^2/\xi+\mathrm{i}0)} \cdot\left[\frac{\eta_{0\mu}\eta_{n\nu}-\eta_{0\nu}\eta_{n\mu}}{2}+\frac{1-\xi}{\xi}\frac{p_0(p_\mu\eta_{n\nu}-p_\nu\eta_{n\mu})}{p^2-\lambda^2/\xi+\mathrm{i}0}\right]. \tag{88}$$

This leads to the following IR-regularized expression for gauge-fixing angular momentum of the electron

$$\langle J^i_\xi \rangle^\lambda_{\mathbf{\Omega}s} = -2\mathrm{i}e_\mathrm{o}^2 s_z \delta^{i3} \cdot \int \frac{d^4p}{(2\pi)^4} \frac{(p_1)^2 + (p_2)^2}{(p^2 - m_\mathrm{o}^2 + \mathrm{i}0)[(p-f)^2 - \lambda^2 + \mathrm{i}0][(p-f)^2 - \lambda^2/\xi + \mathrm{i}0]}. \tag{89}$$

5. Pauli-Villars regularization

We will discuss here implementation of the Pauli-Villars regularization in our calculations (see [19,20] for early works on this technique as well as [18,21] for its variations). In its simplest version, it is based on the following modifications of either fermionic propagator (24)

$$\frac{\gamma \cdot p + m_\mathrm{o}}{p^2 - m_\mathrm{o}^2 + \mathrm{i}0} \to \frac{\gamma \cdot p + m_\mathrm{o}}{p^2 - m_\mathrm{o}^2 + \mathrm{i}0} - \frac{\gamma \cdot p + M}{p^2 - \Lambda^2 + \mathrm{i}0}, \tag{90}$$

where $M = m_\mathrm{o}, \Lambda$, or electromagnetic propagator (25)

$$\frac{d_{\mu\nu}(p)}{p^2 - \lambda^2 + \mathrm{i}0} \to \frac{d_{\mu\nu}(p)}{p^2 - \lambda^2 + \mathrm{i}0} - (\lambda \to \Lambda), \tag{91}$$

where the replacement $\lambda \to \Lambda$ is also applied to $d_{\mu\nu}(p)$, which depends on λ too. The parameter Λ is supposed to be taken to infinity upon removal of the regularization. We have implemented these three ad hoc replacements, finding that none of them leads to total angular momentum of the electron that is independent of ξ. Calculations leading to such a conclusion can be performed by technically straightforward extensions of studies presented in this paper and so we will not linger over them.

Failure of these popular yet somewhat arbitrary regularization attempts means that we need a systematic approach, imposing the Pauli-Villars regularization consistently all across calculations. One may thus consider modifications of the Lagrangian density (see [22,23] for textbook introduction to this technique). Such a bottom-up approach introduces ghost fields, say $\tilde{A}^\mu$ and $\tilde{\psi}$, through the replacement

$$\begin{aligned} \mathcal{L} \to \tilde{\mathcal{L}} = & -\frac{1}{4}F_{\mu\nu}F^{\mu\nu} - \frac{\xi}{2}\left(\partial_\mu A^\mu\right)^2 + \frac{\lambda^2}{2}A_\mu A^\mu + \overline{\psi}\left(\mathrm{i}\gamma^\mu\partial_\mu - m_\mathrm{o}\right)\psi \\ & + \frac{1}{4}\tilde{F}_{\mu\nu}\tilde{F}^{\mu\nu} + \frac{\xi}{2}\left(\partial_\mu \tilde{A}^\mu\right)^2 - \frac{\Lambda^2}{2}\tilde{A}_\mu\tilde{A}^\mu + \overline{\tilde{\psi}}\left(\mathrm{i}\gamma^\mu\partial_\mu - \Lambda\right)\tilde{\psi} \\ & - e_\mathrm{o}(\overline{\psi}\gamma^\mu\psi + \overline{\tilde{\psi}}\gamma^\mu\tilde{\psi})(A_\mu + \tilde{A}_\mu). \end{aligned} \tag{92}$$

This leads to the interaction-picture density of the interaction Hamiltonian

$$\tilde{\mathcal{H}}^I_{\mathrm{int}} = e_\mathrm{o}(:\overline{\psi}_I\gamma^\mu\psi_I: + :\overline{\tilde{\psi}}_I\gamma^\mu\tilde{\psi}_I:)(A^I_\mu + \tilde{A}^I_\mu), \tag{93}$$

which has to be used in imaginary time evolutions. Such evolutions in our studies start from the state

$$|\bullet\rangle = |\mathbf{0}s\rangle \otimes |\tilde{0}\rangle, \tag{94}$$

where $|\tilde{0}\rangle$ contains no ghost particles.

As we discuss in Appendix D, replacements

$$\mathcal{H}^I_{\mathrm{int}} \to \tilde{\mathcal{H}}^I_{\mathrm{int}}, \ |\mathbf{0}s\rangle \to |\bullet\rangle \tag{95}$$

performed on (22) regularize only expectation values of $J^i_{\mathrm{spin}\bullet}$ and $J^i_{\mathrm{orb}\bullet}$. They are equivalent to modification (91) of the electromagnetic propagator in calculations from Secs. 3 and 4.1. The problem now is that replacements (95), when imposed on (22), *do not* regularize expectation values of $J^i_{\mathrm{spin}\sim}$, $J^i_{\mathrm{orb}\sim}$, and J^i_ξ.

To overcome this difficulty, we first introduce ghost angular momentum operators $\tilde{J}^i_\chi$, which are obtained from J^i_χ by replacing all fields with their ghost counterparts. Next, we consider

$$J^i - \tilde{J}^i = \sum_\chi (J^i_\chi - \tilde{J}^i_\chi), \tag{96}$$

where χ is given by (22d). The expectation value of the left-hand side of (96), upon removal of the regularization, should yield total angular momentum of the electron. It should be so because ghost angular momentum should not contribute in such a limit (there are no ghost particles in the unperturbed state of the system and the $\Lambda \to \infty$ limit suppresses addition of such particles to the perturbed state).

The idea now is to compute the expectation value of

$$J^i_\chi - \tilde{J}^i_\chi \tag{97}$$

in the system described by modified Lagrangian density (92), and to treat the resulting expression, say $\langle J^i_\chi \rangle^{\lambda\Lambda}_{\mathbf{\Omega}s}$, as both the IR- and UV-regularized expectation value of the operator J^i_χ. According to remarks presented below (96), such a regularization procedure should not affect the value of total angular momentum of the electron, and so it may be considered as a prospective solution to regularization challenges that we face.

To put such a scheme to the test, we marry up (22) with (95), and replace J^i_χ in the resulting formula by (97) getting

$$\langle J^i_\chi \rangle^{\lambda\Lambda}_{\mathbf{\Omega}s} = \langle J^i_\chi \rangle^{\lambda}_{\mathbf{\Omega}s} - \langle J^i_\chi \rangle^{\Lambda}_{\mathbf{\Omega}s} \tag{98}$$

for all angular momenta that we study (see Appendix D for derivation of this formula). For $\chi = \mathrm{spin}\bullet, \mathrm{orb}\bullet$ this is exactly what one obtains through replacements (95) imposed on (22) because those angular momenta are linear in electromagnetic propagators–see the comment below (95). For $\chi = \mathrm{spin}\sim, \mathrm{orb}\sim, \xi$, (98) does not correspond to any of above-mentioned modifications of propagators. For example, (98) is not equivalent to (91) because expressions for those angular momenta are quadratic in electromagnetic propagators. It is thus evident that such a ghost subtraction technique extends the standard Pauli-Villars approach based solely on modifications of Lagrangian density (92). We find it quite reassuring that these two methods agree for fermionic spin and orbital angular momenta, where the standard approach works.

All in all, (98) delivers the consistent Pauli-Villars regularization of all angular momenta that we study. Such a procedure, when individual regularized angular momenta are added up, leads to the ξ-independent value of total angular momentum of the electron (Sec. 6). It is perhaps worth to stress that the fact that we work with arbitrary $\xi > 0$ allows us for a rather stringent test of reliability of the regularization procedure that we use. Indeed, the requirement of gauge invariance, within the family of all covariant gauges, eliminates a great deal of presumably sensible Pauli-Villars-like regularizations.

6. One-loop radiative corrections

To compute one-loop radiative corrections, we will use subtraction procedure (98) to impose ultraviolet (UV) regularization onto expressions (49), (53), (64), (76), (87), and (89). This step is necessary because without it those expressions do not have definite values. To simplify such obtained formulae, products of propagators' denominators will be joined with the following identities

$$\frac{1}{AB} = \int_0^1 ds \frac{1}{[sA + (1-s)B]^2}, \tag{99a}$$

$$\frac{1}{AB^2} = \int_0^1 ds \frac{2(1-s)}{[sA + (1-s)B]^3}, \tag{99b}$$

$$\frac{1}{A^2B^2} = \int_0^1 ds \frac{6(1-s)s}{[sA + (1-s)B]^4}, \tag{99c}$$

$$\frac{1}{ABC} = \int_0^1 ds \int_0^{1-s} du \frac{2}{[sA + uB + (1-s-u)C]^3}, \tag{99d}$$

the timelike component of the 4-vector p will be shifted to make resulting denominators p^2 dependent, Lorentz averaging of numerators will be implemented through replacements $p_\mu p_\nu \to \eta_{\mu\nu} p^2/4$, and finally Wick rotation will be performed followed by straightforward evaluation of resulting Euclidean integrals. Such obtained expressions will be compactly written after introduction of the following functions

$$\Delta_\chi = (1-s)^2 + s(\chi/m_o)^2, \tag{100}$$

$$\tilde{\Delta}_\chi = (1-s-u)^2 + (s + u/\xi)(\chi/m_o)^2. \tag{101}$$

Above-mentioned calculations will be done under tacit assumptions that these functions are greater than zero for $\chi = \lambda, \Lambda$.

6.1. Fermionic spin angular momentum

We will apply here procedure (98) to individual diagrams introducing

$$\text{Diag. X}|_{\lambda\Lambda} = \text{Diag. X} - (\lambda \to \Lambda) \tag{102}$$

as the Pauli-Villars-regularized version of IR-regularized only Diag. X from Sec. 3. Note that limit (26) is already taken in (102).

Following steps outlined around (99), we get

$$\begin{aligned}\text{Diag. 2a}|_{\lambda\Lambda} = {} & \frac{e_o^2 s_z \delta^{i3}}{8\pi^2} \int_0^1 ds (1-s) \left[\ln \frac{\Delta_\Lambda}{\Delta_\lambda} + (1+s^2)\left(\frac{1}{\Delta_\Lambda} - \frac{1}{\Delta_\lambda}\right)\right] \\ & + \frac{e_o^2 s_z \delta^{i3}}{8\pi^2} \frac{1-\xi}{\xi} \ln \frac{\Lambda}{\lambda}\end{aligned} \tag{103}$$

and

$$\text{Diag. 2b}|_{\lambda\Lambda} + \text{Diag. 2c}|_{\lambda\Lambda} + \text{Diag. 3a}|_{\lambda\Lambda} =$$

$$\frac{e_o^2 s_z \delta^{i3}}{8\pi^2}\int_0^1 ds\left[s\ln\frac{\Delta_\lambda}{\Delta_\Lambda}+2(2-s)(1-s)s\left(\frac{1}{\Delta_\lambda}-\frac{1}{\Delta_\Lambda}\right)\right]-\frac{e_o^2 s_z \delta^{i3}}{8\pi^2}\frac{1-\xi}{\xi}\ln\frac{\Lambda}{\lambda}. \quad (104)$$

Integrals in these equations can be analytically evaluated, but resulting expressions are not compact. We list them in Appendix E. Among other things, they can be used for showing that unless ξ is fine-tuned, (103) and (104) are logarithmically divergent in both IR and UV upon removal of the regularization. For $\xi = \infty$, the Landau gauge, these expressions are still IR divergent but UV finite. For $\xi = 1/3$, the Fried-Yennie gauge, (103) and (104) are IR finite but UV divergent. Both features are typical of covariant gauge calculations.

Next, we take limits of $\lambda \to 0$ and $\Lambda \to \infty$ on the sum of (33), (103), and (104) getting

$$\langle J^i_{\text{spin}\bullet}\rangle_{\mathbf{\Omega}s} = s_z\delta^{i3}\left(1-\frac{e_o^2}{8\pi^2}\right). \quad (105)$$

Using $e_o = e + O(e^3)$, this can be written as

$$\langle J^i_{\text{spin}\bullet}\rangle_{\mathbf{\Omega}s} = s_z\delta^{i3}\left(1-\frac{\alpha}{2\pi}\right)+O(\alpha^2). \quad (106)$$

This one-loop result for fermionic spin angular momentum of the electron agrees with earlier studies [12,13]. Several remarks are in order now.

To begin, our calculations show that (105) is ξ-independent, i.e., one and the same in the family of all covariant gauges. This becomes apparent even before removal of the regularization due to trivial cancellation of last terms in (103) and (104) when the sum of all diagrams is considered. We find it interesting that ξ-dependence in these equations takes such a simple form despite the fact that ξ shows up in the denominator of electromagnetic propagator (25). Indeed, one would naturally expect that after joining propagators' denominators through (99), ξ-dependence will be transferred to the Δ_χ-like function appearing under the integral over the auxiliary parameter s. This is actually what happens in intermediate stages of calculations, but then unforeseen simplifications occur allowing for trivial evaluation of ξ-dependent parts of (103) and (104).

Next, we remark that (104) is equal to $s_z\delta^{i3}(Z_2-1)$, where Z_2 is the renormalization constant of the Dirac field. One can easily verify this statement in the Feynman gauge by looking at Sec. 7.1 of [17], where $Z_2(\xi = 1)$ is computed. In the general covariant gauge, one can repeat calculations from [17] with propagator (25). Such obtained expression for $Z_2(\xi)$ is complicated, but it can be easily numerically checked that it also supports the above remark. Appearance of Z_2 in (104) is expected. For example, a quick look at Figs. 2b, 2c, and 3a reveals that diagrams depicted there are similar in structure to the ones encountered during evaluation of Z_2 from the study of the electron propagator in the QED vacuum state [17]. Finally, we mention that the $\xi \neq 1$ correction to $Z_2(\xi)$, which can be extracted from the last term in (104), appears also in [24], where calculations are Pauli-Villars-regularized in a slightly different way.[5]

6.2. Other angular momenta

We will apply here regularization procedure (98) to angular momenta studied in Sec. 4. This results in the following set of equations

[5] The difference comes from the fact that our regularization is consistently implemented throughout calculations, whereas the one in [24] is done "by hand".

$$\langle J^i_{\mathrm{orb}\bullet}\rangle^{\lambda\Lambda}_{\mathbf{\Omega}s} = -4\mathrm{i}e_{\mathrm{o}}^2 s_z\delta^{i3}\int\frac{d^4p}{(2\pi)^4}\frac{(p_1)^2+(p_2)^2}{(p^2-m_{\mathrm{o}}^2+\mathrm{i}0)^2} \cdot\left[\frac{1}{(p-f)^2-\lambda^2+\mathrm{i}0}\left(1+\frac{1-\xi}{2\xi}\frac{p^2-m_{\mathrm{o}}^2}{(p-f)^2-\lambda^2/\xi+\mathrm{i}0}\right)-(\lambda\to\Lambda)\right], \tag{107}$$

$$\langle J^i_{\mathrm{spin}\sim}\rangle^{\lambda\Lambda}_{\mathbf{\Omega}s} = -4\mathrm{i}e_{\mathrm{o}}^2 s_z\delta^{i3}\int\frac{d^4p}{(2\pi)^4}\frac{2(p^0-m_{\mathrm{o}})^2-(p_1)^2-(p_2)^2}{p^2-m_{\mathrm{o}}^2+\mathrm{i}0} \cdot\left[\frac{1}{[(p-f)^2-\lambda^2+\mathrm{i}0]^2}-(\lambda\to\Lambda)\right], \tag{108}$$

$$\langle J^i_{\mathrm{orb}\sim}\rangle^{\lambda\Lambda}_{\mathbf{\Omega}s} = -4\mathrm{i}e_{\mathrm{o}}^2 s_z\delta^{i3}\int\frac{d^4p}{(2\pi)^4}\frac{(p_1)^2+(p_2)^2}{p^2-m_{\mathrm{o}}^2+\mathrm{i}0} \cdot\left[\frac{1}{[(p-f)^2-\lambda^2+\mathrm{i}0]^2}\left(1-\frac{1}{2\xi}\frac{(p-f)^2-\lambda^2}{(p-f)^2-\lambda^2/\xi+\mathrm{i}0}\right)-(\lambda\to\Lambda)\right], \tag{109}$$

$$\langle J^i_{\xi}\rangle^{\lambda\Lambda}_{\mathbf{\Omega}s} = -2\mathrm{i}e_{\mathrm{o}}^2 s_z\delta^{i3}\int\frac{d^4p}{(2\pi)^4}\frac{(p_1)^2+(p_2)^2}{p^2-m_{\mathrm{o}}^2+\mathrm{i}0} \cdot\left[\frac{1}{[(p-f)^2-\lambda^2+\mathrm{i}0][(p-f)^2-\lambda^2/\xi+\mathrm{i}0]}-(\lambda\to\Lambda)\right]. \tag{110}$$

Even without evaluating these expressions, one can notice that their sum is ξ-independent, which is something that we have anticipated in Sec. 5. A bit surprising now is that $\langle J^i_{\mathrm{spin}\sim}\rangle^{\lambda\Lambda}_{\mathbf{\Omega}s}$ and $\langle J^i_{\mathrm{orb}\bullet}+J^i_{\mathrm{orb}\sim}+J^i_{\xi}\rangle^{\lambda\Lambda}_{\mathbf{\Omega}s}$ are separately ξ-independent. Such an observation, however, is formal because we will shortly see that both quantities are actually infinite upon removal of the regularization.

Following the procedure outlined at the beginning of Sec. 6, we get

$$\langle J^i_{\mathrm{orb}\bullet}\rangle^{\lambda\Lambda}_{\mathbf{\Omega}s} = -s_z\delta^{i3}\frac{e_{\mathrm{o}}^2}{4\pi^2}\int_0^1 ds(1-s)\ln\frac{\Delta_\Lambda}{\Delta_\lambda} - s_z\delta^{i3}\frac{e_{\mathrm{o}}^2}{8\pi^2}\frac{1-\xi}{\xi}\int_0^1 ds\int_0^{1-s}du\ln\frac{\tilde{\Delta}_\Lambda}{\tilde{\Delta}_\lambda}, \tag{111}$$

$$\langle J^i_{\mathrm{spin}\sim}\rangle^{\lambda\Lambda}_{\mathbf{\Omega}s} = s_z\delta^{i3}\frac{e_{\mathrm{o}}^2}{2\pi^2}\int_0^1 ds\, s\left[\ln\frac{\Delta_\Lambda}{\Delta_\lambda}-(1-s)^2\left(\frac{1}{\Delta_\lambda}-\frac{1}{\Delta_\Lambda}\right)\right], \tag{112}$$

$$\langle J^i_{\mathrm{orb}\sim}\rangle^{\lambda\Lambda}_{\mathbf{\Omega}s} = -s_z\delta^{i3}\frac{e_{\mathrm{o}}^2}{4\pi^2}\int_0^1 ds\, s\ln\frac{\Delta_\Lambda}{\Delta_\lambda} + s_z\delta^{i3}\frac{e_{\mathrm{o}}^2}{8\pi^2}\frac{1}{\xi}\int_0^1 ds\int_0^{1-s}du\ln\frac{\tilde{\Delta}_\Lambda}{\tilde{\Delta}_\lambda}, \tag{113}$$

$$\langle J^i_{\xi}\rangle^{\lambda\Lambda}_{\mathbf{\Omega}s} = -s_z\delta^{i3}\frac{e_{\mathrm{o}}^2}{8\pi^2}\int_0^1 ds\int_0^{1-s}du\ln\frac{\tilde{\Delta}_\Lambda}{\tilde{\Delta}_\lambda}. \tag{114}$$

This can be further simplified if we remove the IR regularization. With some extra effort, we get the following results exhibiting rather non-trivial ξ-dependence

$$\lim_{\lambda\to0}\langle J^i_{\mathrm{orb}\bullet}\rangle^{\lambda\Lambda}_{\mathbf{\Omega}s} \simeq s_z\delta^{i3}\frac{e_{\mathrm{o}}^2}{8\pi^2}\left(-\frac{1+\xi}{\xi}\ln\frac{\Lambda}{m_{\mathrm{o}}}+\frac{5}{4}-\frac{3}{4\xi}+\frac{\ln\xi}{2\xi}\right), \tag{115}$$

$$\lim_{\lambda\to0}\langle J^i_{\mathrm{spin}\sim}\rangle^{\lambda\Lambda}_{\mathbf{\Omega}s} \simeq s_z\delta^{i3}\frac{e_{\mathrm{o}}^2}{2\pi^2}\left(\ln\frac{\Lambda}{m_{\mathrm{o}}}+\frac{3}{4}\right), \tag{116}$$

$$\lim_{\lambda\to 0}\langle J^i_{\mathrm{orb}\sim}\rangle^{\lambda\Lambda}_{\mathbf{\Omega}s} \simeq s_z\delta^{i3}\frac{e_o^2}{8\pi^2}\left(\frac{1-2\xi}{\xi}\ln\frac{\Lambda}{m_o}-\frac{5}{2}+\frac{3}{4\xi}-\frac{\ln\xi}{2\xi(1-\xi)}\right), \tag{117}$$

$$\lim_{\lambda\to 0}\langle J^i_{\xi}\rangle^{\lambda\Lambda}_{\mathbf{\Omega}s} \simeq s_z\delta^{i3}\frac{e_o^2}{8\pi^2}\left(-\ln\frac{\Lambda}{m_o}-\frac{3}{4}+\frac{\ln\xi}{2(1-\xi)}\right), \tag{118}$$

where $\simeq$ means that we omit terms that vanish in the limit of $\Lambda\to\infty$. Note that all these expressions are well-defined for any $\xi>0$. Among other things, they allow us to conclude that upon removal of the regularization

$$\langle J^i_{\mathrm{orb}\bullet}+J^i_{\mathrm{spin}\sim}+J^i_{\mathrm{orb}\sim}+J^i_{\xi}\rangle_{\mathbf{\Omega}s} = s_z\delta^{i3}\frac{e_o^2}{8\pi^2}. \tag{119}$$

Combining (119) with (105), we see that in our one-loop calculations the expectation value of total angular momentum operator (18) is given by (29), which can be seen as a self-consistency check of our studies.

7. Discussion

We have teamed the bare perturbative expansion with the imaginary time evolution technique to study radiative corrections to different components of angular momentum of the electron. Our calculations have been done in the general covariant gauge. The results that we have obtained can be summarized as follows.

First, we have carefully discussed implementation of imaginary time evolutions developing a rigorous analytical procedure taking care of singularities that may appear in the course of calculations. Such evolutions are routinely used for generation of ground states, which are then used for computation of expectation values of products of field operators in interacting quantum field theories. Results that we present on this matter are missed in standard textbooks on quantum field theory, where enforcement of the imaginary time limit is trivialized to steps outlined between (27) and (28). On the one hand, our calculations show how disastrous such an oversimplification is when bare perturbation theory is employed for evaluation of self-energy-type diagrams. On the other hand, they provide a general framework that can be readily deployed in computations of other expectation values in quantum field theories. This can be useful for either resolving possible issues with "simplified" handling of the imaginary time limit or for rigorous checking whether such a procedure is justified. These remarks are comprehensively illustrated by our studies in Sec. 3, where computations of some diagrams have been only possible after sophisticated enforcement of the imaginary time limit.

Second, we have computed fermionic spin and orbital, electromagnetic spin and orbital, and gauge-fixing angular momenta of the electron. Out of these five quantities, only fermionic spin angular momentum is gauge invariant, and so it can be conclusively compared to earlier studies, which were done in the light-cone gauge [12,13]. It agrees with these works showing equivalence of the light-cone and general covariant gauge calculations. While such an agreement is expected on general grounds, it is perhaps worth to mention that the issue of gauge independence is still quite non-trivial (Sec. 2.5.2 of [10]). More importantly, technical comparison between calculations in these completely different gauges should be interesting and our detailed discussion should facilitate it.

Third, the remaining four angular momenta are gauge non-invariant. Out of them, gauge-fixing angular momentum is specific to covariant gauge studies and it is instructive to take a closer look at it. It is so because its presence turns out to be of key importance to assigning spin one-half to the electron in covariantly quantized electrodynamics. Indeed, (29) would not hold without it even in the $\xi \to \infty$ limit, where the Lorentz gauge is most transparently enforced (Sec. 15.5 of [25]). This is interesting because J^i_ξ can be seen as a physically meaningless artifact of the quantization procedure and so the question arises why it non-trivially contributes to the physically meaningful quantity such as electron's spin. We expect that resolution of this puzzle is the following. The gauge-fixing term in Lagrangian density (9) not only generates gauge-fixing angular momentum, but it also affects the electromagnetic propagator. The latter impacts computations of expectation values of gauge non-invariant angular momentum operators. As a result, those expectation values get implicitly modified by the presence of the gauge-fixing term and this modification is explicitly cancelled in (29) by gauge-fixing angular momentum, so that it has no effect on electron's spin.

Fourth, we have developed a variant of the Pauli-Villars regularization by requiring that total angular momentum of the electron should be one and the same in the family of all covariant gauges. This obvious condition is violated by the simplest versions of the Pauli-Villars regularization. In our scheme, one subtracts from the observable of interest its ghost operator counterpart, and then calculates the expectation value of such obtained operator through imaginary time evolution. The latter is consistently implemented by the standard addition of ghost fields to the Lagrangian density. The net effect of this procedure is very simple for observables that we study (98). We believe that it would be interesting to put this approach to the test in other problems as well.

Finally, to place result (106) in a wider context, we mention that only one more finite gauge invariant individual component of total angular momentum of the electron was identified so far. Namely, electromagnetic angular momentum [14]

$$\left\langle \int d^3z[\boldsymbol{z} \times (\boldsymbol{E} \times \boldsymbol{B})]^i \right\rangle_{\boldsymbol{\Omega}s} = -s_z \delta^{i3} \frac{\alpha}{2\pi} + O(\alpha^2), \tag{120}$$

where $\boldsymbol{E}$ and $\boldsymbol{B}$ are electric and magnetic field operators.[6] Gauge invariance and finiteness of (106) and (120) should make them especially interesting from the experimental point of view. Given the fact that various angular momenta, contributing to nucleons' spin, have been extensively experimentally studied [15], we are hopeful that such quantities can be also measured. The remaining open question is how this can be achieved.

Declaration of competing interest

The author declares that he has no known competing financial interests or personal relationships that could have appeared to influence the work reported in this paper.

Acknowledgements

I would like to thank Aneta for being a wonderful sounding board during all these studies. Diagrams in this work have been done in JaxoDraw [26]. This work has been supported by the Polish National Science Centre (NCN) grant DEC-2016/23/B/ST3/01152.

[6] Such a result was obtained with ad hoc regularization attempts (90) and (91) explored in [14]. It can be also obtained with the ghost subtraction technique discussed in Sec. 5 and Appendix D of this paper. Its indifference to details of the Pauli-Villars regularization scheme presumably comes from favorable convergence properties of the expression that is regularized during evaluation of (120).

Appendix A. Conventions and all that

We use the Minkowski metric $\eta = \mathrm{diag}(+---)$ and choose $\varepsilon^{0123} = +1 = \varepsilon^{123}$. Greek and Latin indices take values $0, 1, 2, 3$ and $1, 2, 3$, respectively, when they refer to components of 4- and 3-vectors. We use the Einstein summation convention. 3-vectors are written in bold, e.g. $x = (x^\mu) = (x^0, \boldsymbol{x})$. Electron's bare and physical charges are both negative.

We introduce

$$\langle \cdots \rangle_\Psi = \frac{\langle \Psi | \cdots | \Psi \rangle}{\langle \Psi | \Psi \rangle}, \ \omega_{\boldsymbol{q}} = |\boldsymbol{q}|, \ \varepsilon_{\boldsymbol{q}} = \sqrt{m_0^2 + \omega_{\boldsymbol{q}}^2}, \tag{A.1}$$

and write the interaction-picture Dirac field operator as

$$\psi_I(x) = \int \frac{d^3 p}{(2\pi)^{3/2}} \sqrt{\frac{m_0}{\varepsilon_{\boldsymbol{p}}}} \sum_s \Big[a_{\boldsymbol{p}s} u(\boldsymbol{p}, s) e^{-\mathrm{i} p\cdot x} + b^\dagger_{\boldsymbol{p}s} v(\boldsymbol{p}, s) e^{\mathrm{i} p\cdot x} \Big], \tag{A.2a}$$

$$\{a_{\boldsymbol{p}s}, a^\dagger_{\boldsymbol{q}r}\} = \{b_{\boldsymbol{p}s}, b^\dagger_{\boldsymbol{q}r}\} = \delta_{sr}\delta(\boldsymbol{p} - \boldsymbol{q}), \tag{A.2b}$$

where $(p^\mu) = (\varepsilon_{\boldsymbol{p}}, \boldsymbol{p})$, $a_{\boldsymbol{p}s}$ annihilates the electron, and $b_{\boldsymbol{p}s}$ annihilates the positron (both of momentum $\boldsymbol{p}$ and the spin state s). All other anticommutators involving those operators are equal to zero. We choose bispinors $u(\boldsymbol{p}, s)$ and $v(\boldsymbol{p}, s)$, in the standard representation of γ matrices that we use, so that

$$u(\boldsymbol{p}, s) = \frac{1}{\sqrt{2m_0(\varepsilon_{\boldsymbol{p}} + m_0)}} \begin{pmatrix} (\varepsilon_{\boldsymbol{p}} + m_0)\phi^s \\ \boldsymbol{p}\cdot\boldsymbol{\sigma}\phi^s \end{pmatrix}, \tag{A.3a}$$

$$v(\boldsymbol{p}, s) = \frac{1}{\sqrt{2m_0(\varepsilon_{\boldsymbol{p}} - m_0)}} \begin{pmatrix} (\varepsilon_{\boldsymbol{p}} - m_0)\phi^s \\ \boldsymbol{p}\cdot\boldsymbol{\sigma}\phi^s \end{pmatrix}, \tag{A.3b}$$

$$\phi^s = \begin{pmatrix} 1 \\ 0 \end{pmatrix}, \begin{pmatrix} 0 \\ 1 \end{pmatrix}. \tag{A.3c}$$

We define contractions of ψ_I on zero-momentum external lines as

$$\overbrace{\psi_I(x)|\boldsymbol{0}s}\rangle = \frac{u_s}{(2\pi)^{3/2}} e^{-\mathrm{i} f\cdot x}, \ \langle \boldsymbol{0}\overbrace{s|\psi}_I(x) = \frac{\overline{u}_s}{(2\pi)^{3/2}} e^{\mathrm{i} f\cdot x}, \ u_s = u(\boldsymbol{0}, s), \tag{A.4}$$

where $|\boldsymbol{0}s\rangle$ and f are given by (20) and (21), respectively. The u_s bispinors are eigenstates of the z-component of the one-particle fermionic spin angular momentum operator

$$\frac{1}{2}\Sigma^3 u_s = s_z u_s, \ u_s = \begin{pmatrix} 1 \\ 0 \\ 0 \\ 0 \end{pmatrix} \text{ for } s_z = +1/2, \ u_s = \begin{pmatrix} 0 \\ 1 \\ 0 \\ 0 \end{pmatrix} \text{ for } s_z = -1/2. \tag{A.5}$$

Finally, we mention that there is no summation over s in matrix elements $\overline{u}_s \cdots u_s$.

Appendix B. Bispinor matrix elements

Results presented below are obtained in the standard (Dirac) representation of γ matrices. It is then a simple exercise to show that the same results are obtained in all representations unitarily similar to the standard one (Weil, Majorana, etc.). This statement is equivalent to saying that they are invariant under $\gamma^\mu \to U\gamma^\mu U^\dagger$ and $u_s \to U u_s$ transformations, where U is an arbitrary unitary matrix of dimension four (see [27,28] for the discussion of representation-independence of various results associated with the Dirac equation).

The following expressions are used in our computations

$$\overline{u}_s\gamma^\mu(\gamma\cdot p+m_\mathrm{o})\gamma_\mu u_s=4m_\mathrm{o}-2p^0, \tag{B.1}$$

$$\overline{u}_s\gamma\cdot k(\gamma\cdot p+m_\mathrm{o})\gamma\cdot k u_s=2k^0k\cdot p+k^2(m_\mathrm{o}-p^0), \tag{B.2}$$

$$\overline{u}_s\Gamma^i(\gamma^0q^0+m_\mathrm{o})\gamma^\mu(\gamma\cdot p+m_\mathrm{o})\gamma_\mu u_s=s_z\delta^{i3}(m_\mathrm{o}+q^0)\overline{u}_s\gamma^\mu(\gamma\cdot p+m_\mathrm{o})\gamma_\mu u_s, \tag{B.3}$$

$$\overline{u}_s\Gamma^i(\gamma^0q^0+m_\mathrm{o})\gamma\cdot k(\gamma\cdot p+m_\mathrm{o})\gamma\cdot k u_s=s_z\delta^{i3}(m_\mathrm{o}+q^0)\overline{u}_s\gamma\cdot k(\gamma\cdot p+m_\mathrm{o})\gamma\cdot k u_s, \tag{B.4}$$

$$\overline{u}_s\gamma^\mu(\gamma\cdot p+m_\mathrm{o})\Gamma^i(\gamma\cdot p+m_\mathrm{o})\gamma_\mu u_s=2s_z\left[\delta^{i3}(p^2+m_\mathrm{o}^2)+2p_ip_3\right], \tag{B.5}$$

$$\overline{u}_s\gamma\cdot(f-p)(\gamma\cdot p+m_\mathrm{o})\Gamma^i(\gamma\cdot p+m_\mathrm{o})\gamma\cdot(f-p)u_s=s_z\delta^{i3}(p^2-m_\mathrm{o}^2)^2, \tag{B.6}$$

$$\overline{u}_s\gamma^\mu u_s=\eta^{\mu0}, \tag{B.7}$$

$$\varepsilon^{imn}p^n\overline{u}_s\gamma^\mu\{\gamma^m\gamma^0,\gamma\cdot p+m_\mathrm{o}\}\gamma_\mu u_s=-8\mathrm{i}s_z(\delta^{i3}\omega_{\boldsymbol{p}}^2-p_ip_3), \tag{B.8}$$

$$\varepsilon^{imn}p^n\overline{u}_s\gamma\cdot(f-p)\{\gamma^m\gamma^0,\gamma\cdot p+m_\mathrm{o}\}\gamma\cdot(f-p)u_s=-4\mathrm{i}s_z(\delta^{i3}\omega_{\boldsymbol{p}}^2-p_ip_3)(p^2-m_\mathrm{o}^2). \tag{B.9}$$

We mention in passing that we simplify matrix elements (B.5), (B.8), and (B.9) under integral signs by the replacement $p_ip_3\to\delta^{i3}(p_3)^2$.

It is interesting to note that s_z-dependence, in all expectation values that we study, comes from expressions that critically depend on the four-dimensional Levi-Civita symbol, whose extension to a $d\neq4$ dimensional space-time, used in the dimensional regularization, is problematic (see e.g. Appendix B.2 of [29] and references therein). This can be proved by combining (B.7) and the following easy-to-verify identities

$$\overline{u}_s\gamma^\mu\gamma^\nu u_s=\eta^{\mu\nu}-2\mathrm{i}s_z\varepsilon^{0\mu\nu3}, \tag{B.10}$$

$$\overline{u}_s\gamma^\mu\gamma^\sigma\gamma^\nu u_s=\eta^{\mu\sigma}\eta^{\nu0}+\eta^{\sigma\nu}\eta^{\mu0}-\eta^{\mu\nu}\eta^{\sigma0}-2\mathrm{i}s_z\varepsilon^{\mu\sigma\nu3}, \tag{B.11}$$

$$\overline{u}_s\gamma^0\gamma^1\gamma^2\gamma^3u_s=0 \tag{B.12}$$

with the observation that any product of γ matrices can be always reduced to the single term containing at most four γ matrices, whose indices are distinct.

Appendix C. Implementation of imaginary time evolutions

In the following, we work out integrals that are necessary for implementation of imaginary time evolutions. While doing so, we will frequently use the Sochocki-Plemelj formula

$$⨍ dx\frac{f(x)}{x-x_0}=\int dx\left[\pm\mathrm{i}\pi\delta(x-x_0)+\frac{1}{x-x_0\pm\mathrm{i}0}\right]f(x), \tag{C.1}$$

where $⨍$ stands for the Cauchy principal value. Several things have to be kept in mind in the following discussion.

First, as we have mentioned in Sec. 2, T will be greater than zero during evaluation of integrals and then the limit $T\to\infty(1-\mathrm{i}0)$ will be taken.

Second, we will use below the function

$$G(k^0,p^0,\dots), \tag{C.2}$$

which will be assumed to have poles at

$$k^0 = \pm\sqrt{\omega_{\boldsymbol{p}}^2 + M^2} \mp \mathrm{i}0, \;\; p^0 = \pm\sqrt{\omega_{\boldsymbol{p}}^2 + M'^2} \mp \mathrm{i}0, \tag{C.3}$$

etc. Masses M, M', etc. will be greater than zero. In other words, poles of (C.2) will come from propagators' denominators: $(k^0)^2 - \omega_{\boldsymbol{p}}^2 - M^2 + \mathrm{i}0$, $(p^0)^2 - \omega_{\boldsymbol{p}}^2 - M'^2 + \mathrm{i}0$, etc.

Third, as (C.2) will vanish for large arguments in our studies, there will be no problems with convergence of contour integrals that we will discuss.

Type I integrals. The integrals of interest here are given by the formula

$$\chi_\mathrm{I} = \lim_{T\to\infty(1-\mathrm{i}0)} \int dp^0 dk^0 G(k^0, p^0) \frac{\sin^2[T(k^0+p^0-m_\mathrm{o})]}{(k^0+p^0-m_\mathrm{o})^2}, \tag{C.4}$$

where poles of the function G are characterized by $M > 0$ and $M' = m_\mathrm{o}$. Such integrals appear in studies of Diag. 3a, where M is greater than zero due to the IR regularization provided by either the photon mass term or the ghost photon mass term in Pauli-Villars-regularized calculations.

We rewrite (C.4) as

$$\begin{aligned}\chi_\mathrm{I} =& \frac{1}{4} \lim_{T\to\infty(1-\mathrm{i}0)} \int dp^0 dk^0 G(k^0, p^0) \frac{1-e^{2\mathrm{i}T(k^0+p^0-m_\mathrm{o})}}{k^0+p^0-m_\mathrm{o}} \frac{1}{k^0+p^0-m_\mathrm{o}} \\ &+ \frac{1}{4} \lim_{T\to\infty(1-\mathrm{i}0)} \int dp^0 dk^0 G(k^0, p^0) \frac{1-e^{-2\mathrm{i}T(k^0+p^0-m_\mathrm{o})}}{k^0+p^0-m_\mathrm{o}} \frac{1}{k^0+p^0-m_\mathrm{o}}.\end{aligned} \tag{C.5}$$

Using now (C.1), we arrive at

$$\chi_\mathrm{I} = \pi \int dp^0 G(m_\mathrm{o} - p^0, p^0) \lim_{T\to\infty(1-\mathrm{i}0)} T \tag{C.6a}$$

$$+ \frac{1}{4} \lim_{T\to\infty(1-\mathrm{i}0)} \int dp^0 dk^0 G(k^0, p^0) \frac{1-e^{2\mathrm{i}T(k^0+p^0-m_\mathrm{o})}}{k^0+p^0-m_\mathrm{o}} \frac{1}{k^0+p^0-m_\mathrm{o}+\mathrm{i}0} \tag{C.6b}$$

$$+ \frac{1}{4} \lim_{T\to\infty(1-\mathrm{i}0)} \int dp^0 dk^0 G(k^0, p^0) \frac{1-e^{-2\mathrm{i}T(k^0+p^0-m_\mathrm{o})}}{k^0+p^0-m_\mathrm{o}} \frac{1}{k^0+p^0-m_\mathrm{o}-\mathrm{i}0}. \tag{C.6c}$$

Suppose now that we evaluate integrals (C.6b) and (C.6c) on semicircular contours in upper and lower half-planes of complex k^0 and p^0, respectively. This turns exponential terms in (C.6b) and (C.6c) into

$$e^{\pm 2\mathrm{i}T(k^0+p^0-m_\mathrm{o})} \xrightarrow[\text{integrations}]{\text{contour}} e^{-2\mathrm{i}T\gamma_\pm}, \tag{C.7a}$$

$$\gamma_\pm = \sqrt{\omega_{\boldsymbol{p}}^2 + M^2} + \sqrt{\omega_{\boldsymbol{p}}^2 + M'^2} \pm m_\mathrm{o}. \tag{C.7b}$$

Next, we note that $\gamma_\pm > 0$ for M and M' specified below (C.4). Therefore, when we take the limit $T \to \infty(1-\mathrm{i}0)$, exponential terms can be dropped from (C.6b) and (C.6c) if we properly shift poles of $1/(k^0 + p^0 - m_\mathrm{o})$, which amounts to

$$\begin{aligned}\chi_\mathrm{I} =& \pi \int dp^0 G(m_\mathrm{o} - p^0, p^0) \lim_{T\to\infty(1-\mathrm{i}0)} T \\ &+ \frac{1}{4} \int dp^0 dk^0 \left[\frac{G(k^0, p^0)}{(k^0+p^0-m_\mathrm{o}+\mathrm{i}0)^2} + \frac{G(k^0, p^0)}{(k^0+p^0-m_\mathrm{o}-\mathrm{i}0)^2} \right].\end{aligned} \tag{C.8}$$

Type II integrals. Next, we introduce

$$\tilde{G}(k^0, p^0, q^0) = \frac{G(k^0, p^0)}{q^0 - m_\mathrm{o} + \mathrm{i}0}, \tag{C.9}$$

where $G(k^0, p^0)$ is the same as in $\chi_{\rm I}$, and consider

$$\chi_{\rm II} = \lim_{T\to\infty(1-{\rm i}0)} \int dp^0 dk^0 dq^0 \tilde{G}(k^0, p^0, q^0) \frac{\sin[T(k^0+p^0-q^0)]}{k^0+p^0-q^0} \frac{\sin[T(k^0+p^0-m_{\rm o})]}{k^0+p^0-m_{\rm o}}. \tag{C.10}$$

Integrals of such a form appear in studies of Diags. 2b and 2c.

We rewrite (C.10) as

$$\begin{aligned}\chi_{\rm II} =& \frac{1}{4} \lim_{T\to\infty(1-{\rm i}0)} ⨍ dp^0 dk^0 dq^0 \tilde{G}(k^0, p^0, q^0) e^{-{\rm i}T(q^0-m_{\rm o})} \frac{1-e^{2{\rm i}T(k^0+p^0-m_{\rm o})}}{k^0+p^0-m_{\rm o}} \\ &\cdot \frac{1}{k^0+p^0-q^0} \\ &+ \frac{1}{4} \lim_{T\to\infty(1-{\rm i}0)} ⨍ dp^0 dk^0 dq^0 \tilde{G}(k^0, p^0, q^0) e^{{\rm i}T(q^0-m_{\rm o})} \frac{1-e^{-2{\rm i}T(k^0+p^0-m_{\rm o})}}{k^0+p^0-m_{\rm o}} \\ &\cdot \frac{1}{k^0+p^0-q^0}.\end{aligned} \tag{C.11}$$

Employing (C.1), we obtain

$$\begin{aligned}\chi_{\rm II} =& \frac{1}{4} \lim_{T\to\infty(1-{\rm i}0)} \int dp^0 dk^0 dq^0 \tilde{G}(k^0, p^0, q^0) e^{-{\rm i}T(q^0-m_{\rm o})} \frac{1-e^{2{\rm i}T(k^0+p^0-m_{\rm o})}}{k^0+p^0-m_{\rm o}} \\ &\cdot \frac{1}{k^0+p^0-q^0+{\rm i}0} \\ &+ \frac{1}{4} \lim_{T\to\infty(1-{\rm i}0)} \int dp^0 dk^0 dq^0 \tilde{G}(k^0, p^0, q^0) e^{{\rm i}T(q^0-m_{\rm o})} \frac{1-e^{-2{\rm i}T(k^0+p^0-m_{\rm o})}}{k^0+p^0-m_{\rm o}} \\ &\cdot \frac{1}{k^0+p^0-q^0+{\rm i}0}.\end{aligned} \tag{C.12}$$

Doing the first (second) integral over q^0 on the lower (upper) semicircular contour of the complex q^0 half-plane, joining integrals, rearranging terms, and then splitting them again we arrive at

$$\begin{aligned}\chi_{\rm II} =& -\frac{{\rm i}\pi}{2} \lim_{T\to\infty(1-{\rm i}0)} ⨍ dp^0 dk^0 G(k^0, p^0) \frac{e^{{\rm i}T(k^0+p^0-m_{\rm o})} - e^{2{\rm i}T(k^0+p^0-m_{\rm o})}}{k^0+p^0-m_{\rm o}} \frac{1}{k^0+p^0-m_{\rm o}} \\ &- \frac{{\rm i}\pi}{2} \lim_{T\to\infty(1-{\rm i}0)} ⨍ dp^0 dk^0 G(k^0, p^0) \frac{1-e^{-{\rm i}T(k^0+p^0-m_{\rm o})}}{k^0+p^0-m_{\rm o}} \frac{1}{k^0+p^0-m_{\rm o}}.\end{aligned} \tag{C.13}$$

Using again (C.1), we obtain

$$\begin{aligned}\chi_{\rm II} =& -{\rm i}\pi^2 \int dp^0 G(m_{\rm o}-p^0, p^0) \lim_{T\to\infty(1-{\rm i}0)} T \\ &- \frac{{\rm i}\pi}{2} \lim_{T\to\infty(1-{\rm i}0)} \int dp^0 dk^0 G(k^0, p^0) \frac{e^{{\rm i}T(k^0+p^0-m_{\rm o})} - e^{2{\rm i}T(k^0+p^0-m_{\rm o})}}{k^0+p^0-m_{\rm o}} \\ &\cdot \frac{1}{k^0+p^0-m_{\rm o}+{\rm i}0} \\ &- \frac{{\rm i}\pi}{2} \lim_{T\to\infty(1-{\rm i}0)} \int dp^0 dk^0 G(k^0, p^0) \frac{1-e^{-{\rm i}T(k^0+p^0-m_{\rm o})}}{k^0+p^0-m_{\rm o}} \frac{1}{k^0+p^0-m_{\rm o}-{\rm i}0}.\end{aligned} \tag{C.14}$$

Repeating now steps around (C.7), we note that exponential terms in (C.14) vanish upon taking the limit, which after proper shifting of the pole of $1/(k^0 + p^0 - m_o)$ leaves us with

$$\chi_{\rm II} = -i\pi^2 \int dp^0 G(m_o - p^0, p^0) \lim_{T\to\infty(1-i0)} T - \frac{i\pi}{2} \int dp^0 dk^0 \frac{G(k^0, p^0)}{(k^0 + p^0 - m_o - i0)^2}. \tag{C.15}$$

Type III integrals. Now, we consider

$$\chi_{\rm III} = \lim_{T\to\infty(1-i0)} \int dp^0 dk^0 dq^0 G(k^0, p^0, q^0) \frac{\sin[T(k^0 + p^0 - m_o)]}{k^0 + p^0 - m_o} \frac{\sin[T(k^0 + q^0 - m_o)]}{k^0 + q^0 - m_o}, \tag{C.16}$$

where poles of $G(k^0, p^0, q^0)$ are parameterized by $M > 0$ and $M' = M'' = m_o$ in expressions for Diags. 2a and 4a. During evaluation of electromagnetic spin, electromagnetic orbital, and gauge-fixing angular momenta, they are given by $M = m_o$, and $M', M'' > 0$.

We rewrite (C.16) as

$$\begin{aligned}\chi_{\rm III} =& \frac{1}{2i} \lim_{T\to\infty(1-i0)} ⨍ dp^0 dk^0 dq^0 G(k^0, p^0, q^0) \frac{\sin[T(k^0 + p^0 - m_o)]}{k^0 + p^0 - m_o} \frac{e^{iT(k^0+q^0-m_o)}}{k^0 + q^0 - m_o} \\ &- \frac{1}{2i} \lim_{T\to\infty(1-i0)} ⨍ dp^0 dk^0 dq^0 G(k^0, p^0, q^0) \frac{\sin[T(k^0 + p^0 - m_o)]}{k^0 + p^0 - m_o} \frac{e^{-iT(k^0+q^0-m_o)}}{k^0 + q^0 - m_o},\end{aligned} \tag{C.17}$$

which after using (C.1) leads to

$$\begin{aligned}\chi_{\rm III} = &\pi \lim_{T\to\infty(1-i0)} \int dp^0 dq^0 G(m_o - q^0, p^0, q^0) \frac{\sin[T(p^0 - q^0)]}{p^0 - q^0} \\ &+ \frac{1}{2i} \lim_{T\to\infty(1-i0)} \int dp^0 dk^0 dq^0 G(k^0, p^0, q^0) \frac{\sin[T(k^0 + p^0 - m_o)]}{k^0 + p^0 - m_o} \\ &\cdot \left[\frac{e^{iT(k^0+q^0-m_o)}}{k^0 + q^0 - m_o + i0} - \frac{e^{-iT(k^0+q^0-m_o)}}{k^0 + q^0 - m_o - i0} \right].\end{aligned} \tag{C.18}$$

After splitting integrals over sinuses into Cauchy principal value integrals and then one more employment of (C.1), we obtain

$$\chi_{\rm III} = \pi^2 \int dp^0 G(m_o - p^0, p^0, p^0) \tag{C.19a}$$

$$+ \frac{\pi}{2i} \lim_{T\to\infty(1-i0)} \int dp^0 dq^0 \Big[G(m_o - q^0, p^0, q^0) + G(m_o - p^0, p^0, q^0) \Big] \frac{e^{iT(p^0-q^0)}}{p^0 - q^0 + i0} \tag{C.19b}$$

$$+ \frac{\pi}{2i} \lim_{T\to\infty(1-i0)} \int dp^0 dq^0 \Big[G(m_o - q^0, p^0, q^0) + G(m_o - p^0, p^0, q^0) \Big] \frac{e^{iT(q^0-p^0)}}{q^0 - p^0 + i0} \tag{C.19c}$$

$$- \frac{1}{4} \lim_{T\to\infty(1-i0)} \int dp^0 dk^0 dq^0 G(k^0, p^0, q^0) \frac{e^{iT(2k^0+p^0+q^0-2m_o)}}{(k^0 + p^0 - m_o + i0)(k^0 + q^0 - m_o + i0)} \tag{C.19d}$$

$$-\frac{1}{4}\lim_{T\to\infty(1-\mathrm{i}0)}\int dp^0dk^0dq^0G(k^0,p^0,q^0)\frac{e^{-\mathrm{i}T(2k^0+p^0+q^0-2m_\mathrm{o})}}{(k^0+p^0-m_\mathrm{o}-\mathrm{i}0)(k^0+q^0-m_\mathrm{o}-\mathrm{i}0)} \tag{C.19e}$$

$$+\frac{1}{4}\lim_{T\to\infty(1-\mathrm{i}0)}\int dp^0dk^0dq^0G(k^0,p^0,q^0)\frac{e^{\mathrm{i}T(p^0-q^0)}}{(k^0+p^0-m_\mathrm{o}+\mathrm{i}0)(k^0+q^0-m_\mathrm{o}-\mathrm{i}0)} \tag{C.19f}$$

$$+\frac{1}{4}\lim_{T\to\infty(1-\mathrm{i}0)}\int dp^0dk^0dq^0G(k^0,p^0,q^0)\frac{e^{\mathrm{i}T(q^0-p^0)}}{(k^0+p^0-m_\mathrm{o}-\mathrm{i}0)(k^0+q^0-m_\mathrm{o}+\mathrm{i}0)}. \tag{C.19g}$$

Integrands in terms (C.19b)–(C.19g) involve factors

$$\frac{e^{\pm\mathrm{i}Th^0+\cdots}}{\cdots+h^0\pm\mathrm{i}0}, \tag{C.20}$$

where h^0 variables are timelike components of 4-momenta appearing in expressions for propagators. If we now integrate each term on semicircular contours in upper $(+)$ and lower $(-)$ half-planes of complex h^0, we will see that poles of (C.20) do not contribute to such contour integrals. Thus, only poles of the G function contribute, but they turn exponential terms into the form similar to (C.7). For M, M', and M'' listed below (C.16), one can then easily argue that (C.19b)–(C.19g) are removed by the limit $T\to\infty(1-\mathrm{i}0)$.

All in all, we get

$$\chi_{\mathrm{III}}=\pi^2\int dp^0G(m_\mathrm{o}-p^0,p^0,p^0). \tag{C.21}$$

Appendix D. Pauli-Villars regularization

We will discuss here technicalities related to implementation of the Pauli-Villars regularization through introduction of ghost fields, whose interaction-picture propagators are [23]

$$\tilde{S}(x-y)=\langle\tilde{0}|\mathbb{T}\tilde{\psi}_I(x)\overline{\tilde{\psi}}_I(y)|\tilde{0}\rangle=\mathrm{i}\int\frac{d^4p}{(2\pi)^4}\frac{\gamma\cdot p+\Lambda}{p^2-\Lambda^2+\mathrm{i}0}e^{-\mathrm{i}p\cdot(x-y)}, \tag{D.1}$$

$$\begin{aligned}\tilde{D}_{\mu\nu}(x-y)&=\langle\tilde{0}|\mathbb{T}\tilde{A}^I_\mu(x)\tilde{A}^I_\nu(y)|\tilde{0}\rangle\\&=\mathrm{i}\int\frac{d^4p}{(2\pi)^4}\frac{e^{-\mathrm{i}p\cdot(x-y)}}{p^2-\Lambda^2+\mathrm{i}0}\left(\eta_{\mu\nu}+\frac{1-\xi}{\xi}\frac{p_\mu p_\nu}{p^2-\Lambda^2/\xi+\mathrm{i}0}\right).\end{aligned} \tag{D.2}$$

A quick look at (24) and (25) reveals that while $S(x-y)$ and $\tilde{S}(x-y)$ differ only in masses, $D_{\mu\nu}(x-y)$ and $\tilde{D}_{\mu\nu}(x-y)$ differ in both masses and overall signs.

Modification of (22) by (95) asks for evaluation of

$$\langle\bullet|\mathbb{T}O_I\tilde{\mathcal{H}}^I_{\mathrm{int}}(x)\tilde{\mathcal{H}}^I_{\mathrm{int}}(y)|\bullet\rangle=e_\mathrm{o}^2\mathcal{M}_E\mathcal{M}_D, \tag{D.3}$$

where matrix elements involving either real or ghost electromagnetic (Dirac field) operators are denoted as $\mathcal{M}_E$ ($\mathcal{M}_D$). Their indices are suppressed for the sake of brevity. Expressions for $\mathcal{M}_E$ and $\mathcal{M}_D$ can be easily derived with the help of Wick's theorem. During their evaluation, one must keep in mind that ghost fields follow bosonic statistics. Moreover, it is worth to remember that operators O_I are normal ordered (the same comment applies to their ghost counterparts $\tilde{O}_I$ and to $\tilde{\mathcal{H}}^I_{\mathrm{int}}$). Normal ordering of all these operators substantially simplifies resulting expressions.

Dirac field operators. Taking $O = J^i_{\text{spin}\bullet}, J^i_{\text{orb}\bullet}$, we obtain

$$\mathcal{M}_E = D_{\mu\nu}(x-y) + \tilde{D}_{\mu\nu}(x-y), \tag{D.4}$$

$$\begin{aligned}\mathcal{M}_D =& \langle \mathbf{0}s|\mathbb{T}O_I :\overline{\psi}_I(x)\gamma^\mu\psi_I(x)::\overline{\psi}_I(y)\gamma^\nu\psi_I(y): |\mathbf{0}s\rangle \\ &+\langle \mathbf{0}s|O_I|\mathbf{0}s\rangle \mathrm{Tr}\Big[\tilde{S}(y-x)\gamma^\mu\tilde{S}(x-y)\gamma^\nu\Big].\end{aligned} \tag{D.5}$$

These two formulae also hold when the unit operator is substituted for O. This observation is useful during studies of fermionic spin angular momentum of the electron, where the denominator of (22b) non-trivially contributes.

Electromagnetic operators. For $O = J^i_{\text{spin}\sim}, J^i_{\text{orb}\sim}, J^i_\xi$, we get

$$\mathcal{M}_E = \langle 0|\mathbb{T}O_I A^I_\mu(x)A^I_\nu(y)|0\rangle, \tag{D.6}$$

$$\mathcal{M}_D = \mathcal{F}^{\mu\nu}(x,y) + V\mathrm{Tr}\Big[\tilde{S}(y-x)\gamma^\mu\tilde{S}(x-y)\gamma^\nu\Big], \tag{D.7}$$

where $\mathcal{F}^{\mu\nu}$ is given by (72). Note that the last term of (D.7) is s_z-independent, and so it has no influence on angular momentum of the electron due to reasons explained below (29).

Having these results, one can easily show that replacements (95), when performed on (22), lead to

$$\langle J^i_\chi\rangle^\lambda_{\mathbf{\Omega}s} \to \langle J^i_\chi\rangle^\lambda_{\mathbf{\Omega}s} - \langle J^i_\chi\rangle^\Lambda_{\mathbf{\Omega}s} \;\text{ for }\; \chi = \text{spin}\bullet, \text{orb}\bullet, \tag{D.8}$$

$$\langle J^i_\chi\rangle^\lambda_{\mathbf{\Omega}s} \to \langle J^i_\chi\rangle^\lambda_{\mathbf{\Omega}s} \;\text{ for }\; \chi = \text{spin}\sim, \text{orb}\sim, \xi, \tag{D.9}$$

where the superscript λ reminds us that before introduction of ghost fields our calculations have already been IR-regularized. Thus, while angular momenta listed in (D.8) are regularized by modification (92) of the Lagrangian density, the ones from (D.9) are not. We mention in passing that (D.8) follows from the fact that (D.4) can be written as $D_{\mu\nu}(x-y) - (\lambda \to \Lambda)$.

To fix the problem caused by (D.9), we consider expectation values of differences of angular momentum operators and their ghost counterparts. This asks for evaluation of the analog of (D.3),

$$\langle \bullet|\mathbb{T}\tilde{O}_I\tilde{\mathcal{H}}^I_{\text{int}}(x)\tilde{\mathcal{H}}^I_{\text{int}}(y)|\bullet\rangle = e_0^2\tilde{\mathcal{M}}_E\tilde{\mathcal{M}}_D, \tag{D.10}$$

leading to the following set of expressions.

Ghost Dirac field operators. Taking $\tilde{O} = \tilde{J}^i_{\text{spin}\bullet}, \tilde{J}^i_{\text{orb}\bullet}$, we obtain

$$\tilde{\mathcal{M}}_E = D_{\mu\nu}(x-y) + \tilde{D}_{\mu\nu}(x-y), \tag{D.11}$$

$$\begin{aligned}\tilde{\mathcal{M}}_D =& \frac{\eta^{\mu 0}}{(2\pi)^3}\langle\tilde{0}|\mathbb{T}\tilde{O}_I :\overline{\tilde{\psi}}_I(y)\gamma^\nu\tilde{\psi}_I(y): |\tilde{0}\rangle \\ &+\frac{\eta^{\nu 0}}{(2\pi)^3}\langle\tilde{0}|\mathbb{T}\tilde{O}_I :\overline{\tilde{\psi}}_I(x)\gamma^\mu\tilde{\psi}_I(x): |\tilde{0}\rangle \\ &+V\langle\tilde{0}|\mathbb{T}\tilde{O}_I :\overline{\tilde{\psi}}_I(x)\gamma^\mu\tilde{\psi}_I(x)::\overline{\tilde{\psi}}_I(y)\gamma^\nu\tilde{\psi}_I(y): |\tilde{0}\rangle,\end{aligned} \tag{D.12}$$

where we have used (A.4) and (B.7) to arrive at (D.12).

Ghost electromagnetic operators. For $\tilde{O} = \tilde{J}^i_{\text{spin}\sim}, \tilde{J}^i_{\text{orb}\sim}, \tilde{J}^i_\xi$, we get

$$\tilde{\mathcal{M}}_E = \langle\tilde{0}|\mathbb{T}\tilde{O}_I \tilde{A}^I_\mu(x)\tilde{A}^I_\nu(y)|\tilde{0}\rangle, \tag{D.13}$$

$$\tilde{\mathcal{M}}_D = \mathcal{F}^{\mu\nu}(x,y) + V\mathrm{Tr}\Big[\tilde{S}(y-x)\gamma^\mu\tilde{S}(x-y)\gamma^\nu\Big]. \tag{D.14}$$

Using (D.3)–(D.7) and (D.10)–(D.14), one can show that if we impose on (22) replacements

$$J_\chi^i \to J_\chi^i - \tilde{J}_\chi^i \tag{D.15}$$

and (95), then such modifications will result in

$$\langle J_\chi^i \rangle_{\mathbf{\Omega}s}^{\lambda} \to \langle J_\chi^i \rangle_{\mathbf{\Omega}s}^{\lambda} - \langle J_\chi^i \rangle_{\mathbf{\Omega}s}^{\Lambda} \quad \text{for} \quad \chi = \text{spin}\bullet, \text{orb}\bullet, \text{spin}\sim, \text{orb}\sim, \xi. \tag{D.16}$$

Two comments are in order now.

First, ghost operator subtraction (D.15) does not affect expectation values of angular momentum operators built of Dirac fields, which are regularized by mere addition of ghost fields to the Lagrangian density, see (D.8). The easiest way to see this is to combine the observation that whole (D.12) is s_z-independent with arguments presented below (29).

Second, ghost operator subtraction (D.15) leads to regularization of angular momentum operators composed of electromagnetic operators, for which (D.16) can be understood by noting that (D.13) is obtained by performing the transformation $\lambda \to \Lambda$ on (D.6).

Appendix E. Evaluation of integrals

We evaluate here definite integrals from (103) and (104). To this aim, we need the following indefinite integrals

$$\begin{aligned}
4\int ds(1-s)\left(\ln\Delta_\chi + \frac{1+s^2}{\Delta_\chi}\right) \\
= 2s(\tilde{\chi}^2-4) - \left[(\tilde{\chi}^2-2)^2 + 2(1-s)^2\right]\ln\left[(1-s)^2 + s\tilde{\chi}^2\right] \\
+ \frac{2\tilde{\chi}(\tilde{\chi}^4 - 6\tilde{\chi}^2 + 12)}{\sqrt{4-\tilde{\chi}^2}} \arctan\frac{\tilde{\chi}^2 - 2(1-s)}{\tilde{\chi}\sqrt{4-\tilde{\chi}^2}} + \text{const}
\end{aligned} \tag{E.1}$$

and

$$\begin{aligned}
4\int ds\left(s\ln\Delta_\chi + \frac{2(2-s)(1-s)s}{\Delta_\chi}\right) \\
= 2s(s - 3\tilde{\chi}^2 - 6) + (3\tilde{\chi}^4 + 2s^2 - 6)\ln\left[(1-s)^2 + s\tilde{\chi}^2\right] \\
- \frac{6\tilde{\chi}(\tilde{\chi}^4 - 2\tilde{\chi}^2 - 4)}{\sqrt{4-\tilde{\chi}^2}} \arctan\frac{\tilde{\chi}^2 - 2(1-s)}{\tilde{\chi}\sqrt{4-\tilde{\chi}^2}} + \text{const},
\end{aligned} \tag{E.2}$$

where $\tilde{\chi} = \chi/m_0$.

These expressions can be used for any $0 < \tilde{\chi}^2 < 4$. For $\tilde{\chi}^2 > 4$, the following replacements

$$\sqrt{4-\tilde{\chi}^2} \to \mathrm{i}\sqrt{\tilde{\chi}^2 - 4}, \tag{E.3}$$

$$\arctan\frac{\tilde{\chi}^2 - 2(1-s)}{\tilde{\chi}\sqrt{4-\tilde{\chi}^2}} \to -\mathrm{i}\,\mathrm{arctanh}\frac{\tilde{\chi}^2 - 2(1-s)}{\tilde{\chi}\sqrt{\tilde{\chi}^2-4}} \tag{E.4}$$

should be employed. They make right-hand sides of (E.1) and (E.2) real. Analogical replacements are also meant to be applied below.

Using (E.1) and (E.2), we find

$$\int_0^1 ds(1-s)\left[\ln\frac{\Delta_\Lambda}{\Delta_\lambda}+(1+s^2)\left(\frac{1}{\Delta_\Lambda}-\frac{1}{\Delta_\lambda}\right)\right]=I_1(\tilde{\lambda})-I_1(\tilde{\Lambda})-2\ln\frac{\Lambda}{\lambda}, \tag{E.5a}$$

$$I_1(x)=\frac{x^2-4}{2}(x^2\ln x-1)-\frac{x^4-6x^2+12}{2}\frac{x}{\sqrt{4-x^2}}\arctan\frac{\sqrt{4-x^2}}{x} \tag{E.5b}$$

and

$$\int_0^1 ds\left[s\ln\frac{\Delta_\lambda}{\Delta_\Lambda}+2(2-s)(1-s)s\left(\frac{1}{\Delta_\lambda}-\frac{1}{\Delta_\Lambda}\right)\right]=I_2(\tilde{\lambda})-I_2(\tilde{\Lambda})+2\ln\frac{\Lambda}{\lambda}, \tag{E.6a}$$

$$I_2(x)=\frac{3x^2}{2}(x^2\ln x-1)-\frac{3(x^4-2x^2-4)}{2}\frac{x}{\sqrt{4-x^2}}\arctan\frac{\sqrt{4-x^2}}{x}, \tag{E.6b}$$

respectively.

References

[1] J.J. Thomson, Cathode rays, Philos. Mag. 44 (1897) 293.
[2] G.E. Uhlenbeck, S. Goudsmit, Spinning electrons and the structure of spectra, Nature 117 (1926) 264.
[3] T. Preston, Radiation phenomena in a strong magnetic field, Sci. Trans. Royal Dublin Soc. 6 (1898) 385.
[4] P.A.M. Dirac, The quantum theory of the electron, Proc. R. Soc. A 117 (1928) 610.
[5] J. Schwinger, On quantum-electrodynamics and the magnetic moment of the electron, Phys. Rev. 73 (1948) 416.
[6] J.E. Nafe, E.B. Nelson, The hyperfine structure of hydrogen and deuterium, Phys. Rev. 73 (1948) 718.
[7] H.M. Foley, P. Kusch, On the intrinsic moment of the electron, Phys. Rev. 73 (1948) 412.
[8] E.D. Commins, Electron spin and its history, Annu. Rev. Nucl. Part. Sci. 62 (2012) 133.
[9] R. Greiner, J. Reinhardt, Field Quantization, Springer-Verlag, 1996.
[10] E. Leader, C. Lorcé, The angular momentum controversy: what's it all about and does it matter?, Phys. Rep. 541 (2014) 163;
E. Leader, C. Lorcé, Phys. Rep. 802 (2019) 23, Erratum.
[11] M. Burkardt, H. BC, Angular momentum decomposition for an electron, Phys. Rev. D 79 (2009) 071501(R).
[12] T. Liu, B.-Q. Ma, Angular momentum decomposition from a QED example, Phys. Rev. D 91 (2015) 017501.
[13] X. Ji, A. Schäfer, F. Yuan, J.-H. Zhang, Y. Zhao, Spin decomposition of the electron in QED, Phys. Rev. D 93 (2016) 054013.
[14] B. Damski, Electromagnetic angular momentum of the electron: one-loop studies, Nucl. Phys. B 949 (2019) 114828.
[15] A. Deur, S.J. Brodsky, G.F. de Téramond, The spin structure of the nucleon, Rep. Prog. Phys. 82 (2019) 076201.
[16] R. Jaffe, A. Manohar, The g_1 problem: deep inelastic electron scattering and the spin of the proton, Nucl. Phys. B 337 (1990) 509.
[17] M.E. Peskin, D.V. Schroeder, An Introduction to Quantum Field Theory, Westview Press, 1995.
[18] B.G.-g. Chen, D. Derbes, D. Griffiths, B. Hill, R. Sohn, Y.-S. Ting, Lectures of Sidney Coleman on Quantum Field Theory, World Scientific, 2018.
[19] J. Rayski, Polarization of the vacuum, Phys. Rev. 75 (1949) 1961.
[20] W. Pauli, F. Villars, On the invariant regularization in relativistic quantum theory, Rev. Mod. Phys. 21 (1949) 434.
[21] N.N. Bogolubov, D.V. Shirkov, Introduction to the Theory of Quantized Fields, Interscience Publishers, 1959.
[22] M.D. Schwartz, Quantum Field Theory and the Standard Model, Cambridge University Press, 2015.
[23] S.N. Gupta, Quantum Electrodynamics, Gordon and Breach Science Publishers, 1977.
[24] K. Johnson, B. Zumino, Gauge dependence of the wave-function renormalization constant in quantum electrodynamics, Phys. Rev. Lett. 3 (1959) 351.
[25] S. Weinberg, The Quantum Theory of Fields, Vol. II: Modern Applications, Cambridge University Press, 1996.
[26] D. Binosi, J. Collins, C. Kaufhold, L. Theussl, Jaxodraw: a graphical user interface for drawing Feynman diagrams. Version 2.0 release notes, Comput. Phys. Commun. 180 (2009) 1709.

[27] P.B. Pal, Representation-independent manipulations with Dirac matrices and spinors, arXiv:physics/0703214.

[28] M. Arminjon, F. Reifler, Dirac equation: representation independence and tensor transformation, Braz. J. Phys. 38 (2008) 248.

[29] H.K. Dreiner, H.E. Haber, S.P. Martin, Two-component spinor techniques and Feynman rules for quantum field theory and supersymmetry, Phys. Rep. 494 (2010) 1.